2023

Thermal Management Strategies for Hypersonic Flight: Supercritical CO2 Jet Impingement Cooling Investigation for Leading Edge

Manoj Prabakar Sargunaraj
University of Central Florida

THERMAL MANAGEMENT STRATEGIES FOR HYPERSONIC FLIGHT: SUPERCRITICAL CO_2 JET IMPINGEMENT COOLING INVESTIGATION FOR LEADING EDGE

by

MANOJ PRABAKAR SARGUNARAJ
B.S. Aero-Mechanical Engineering, Aeronautical Society of India, 2014
MS (by research) Aerospace Engineering, Indian Institute of Technology, Madras. 2018
MS Mechanical Engineering, University of Central Florida. 2021

A dissertation submitted in partial fulfillment of the requirements.
for the degree of Doctor of Philosophy
in the Department of Mechanical and Aerospace Engineering
in the College of Engineering and Computer Science
at the University of Central Florida
Orlando, Florida

Fall Term
2023.

Major Professor: Jayanta Kapat

ABSTRACT

This study addresses the critical need for effective thermal management in hypersonic vehicles facing intense heat at their leading edge due to high enthalpy flow. The objective is to propose an active impingement cooling system that ensures the structural stability and performance of these vehicles. This dissertation presents an in-depth exploration of the numerical simulations conducted on the hypersonic leading edge, focusing on a 3mm radius with active cooling utilizing supercritical carbon dioxide (sCO2) as the coolant. The research incorporates conjugate simulations that merge external hypersonic flow and sCO2 active cooling. Utilizing a thermodynamic non-equilibrium two-temperature model and various chemical models, including the 5-species Park's model and the 11-species Gupta's model, separate validations for the external hypersonic flow and internal sCO2 coolant flow were conducted. These validations facilitated combined simulations, underscoring the potential of maintaining metal temperatures within operational limits using sCO2 coolant. A comparative study of the 5-species Park model and 11-species Gupta model demonstrated the former's effectiveness in predicting flow fields at Mach 7. Furthermore, this study shows the effect of varying the coolant tube-to-leading-edge distance (H/D), Thermal barrier coating thickness and impingement angles, demonstrating improved heat transfer performance through these variations.

A key aspect of this work is the exploration of converting hypersonic vehicle heat flux to power using the sCO2 cycle. The conceptual study, illustrated through the Mach 7 case, confirms the feasibility of harnessing power from aerodynamic heat flux, marking a significant progression in the field. This research contributes to the field by offering a detailed analysis of active impingement cooling for hypersonic leading edges, integrating real gas effects and multiple chemical models. The study adds novelty by investigating heat transfer enhancements through

geometric variations and evaluating sCO2's potential as a coolant, addressing key facets of hypersonic vehicle thermal management.

In memory of my father, Sargunaraj, whose patience, and unwavering faith on me continue to fuel my dreams. To my mother, Vijaya, and my brother, Sathish, your enduring love and unwavering support illuminate my path. And to Nandhini, the love of my life, your unwavering belief infuses my days with warmth and purpose.

ACKNOWLEDGMENTS

I extend my heartfelt gratitude to my thesis advisor, Prof. Jayanta Kapat, and the esteemed members of the dissertation committee, Prof. Bhimsen Shivmoggi, and Prof. Kareem Ahmed. Their valuable time spent reviewing my progress and insightful suggestions have been instrumental in shaping this work. A special acknowledgment goes to Dr. Erik Fernandez, whose commitment as a committee member and day-to-day guidance played a pivotal role in my journey. I would like to express my gratitude to ANSYS and its members, particularly Dr. Valerio, Dr. Stefano, and Dr. Swathi, for their valuable contributions during my research and collaboration.

I also wish to express my sincere appreciation to Prof. Gou, the Program Coordinator, and Prof. Peles, the Chair of the Department of Mechanical and Aerospace Engineering, along with all the faculty members, for their timely support. Gratitude is also extended to Dr. Mansy (7 semesters), Dr. Sagnik (1 semester), and Dr. Mitra (1 semester) for granting me the opportunity to contribute as a Graduate Teaching Assistant.

My thanks extend to the entire staff and technical personnel of the Mechanical and Aerospace Engineering Department, with special mention to Gabriela, Amanda, Lynn, Patty, and Kamryn, whose efforts and assistance were consistently unwavering. I appreciate the guidance provided by the UCF Graduate office personnel and the thesis editors throughout this academic journey.

I am deeply indebted to the scholars and fellow students whose insights and suggestions enriched my work. Special thanks to my colleagues in the CATER lab, particularly Dr.Patrick, Immanuel, Dr. Marcel, and Dr. Ladislav. I would also like to express gratitude to my friends, Sankar, Viswa, Vasanth, and Anto, who brought entertainment and fitness through our

participation in the UCF Knights cricket team for three sessions of Central Florida tournaments. Weekends spent playing cricket became a source of refreshment and motivation for my PhD pursuits. Also, I extend my appreciation to my friends from the Lake Mary Legends Cricket team and friends, including Ramesh, Kamesh, Jimmy, Elango S, Uma, Vijay, Attorney Ram, and others. I would also like to express my gratitude to other family members, such as my uncle John and aunt Sakthi from New Jersey, and uncles Suresh, Jeba, Anand, Sampath and Prem. Special thanks to my mother-in-law, Prema Raju, for her unwavering support during my dissertation journey and for taking care of my beloved daughter, Arya. I would also like to extend my thanks to my school and college friends, with a special mention for my friend Ram. I am deeply grateful to my school friend Narayanan, who took care of my father during his illness and funeral in my absence, stepping in for me. To those friends inadvertently omitted here, I sincerely apologize and express my heartfelt gratitude for their love, patience, and understanding throughout this journey.

TABLE OF CONTENTS

LIST OF FIGURES

LIST OF TABLES

NOMENCLATURE

Cp	=	Specific heat, in J/kg/K
d	=	coolant jet diameter
E	=	Total energy
H	=	Total Enthalpy
k	=	Thermal conductivity
Nu	=	Local Nusselt number
Nu’	=	Nusselt number based on adiabatic wall conditions
Ma	=	Mach Number
Re	=	Reynolds number
P	=	Pressure
T	=	Temperature
To	=	Freestream total temperature (K)
T∞	=	Freestream static temperature (K)
Ttr	=	Translational-rotational static temperature (K)
Tve	=	Vibrational-electronic static temperature (K)

TBC = Thermal Barrier Coating

TPS = Thermal Protection System

y+ = Nondimensional wall distance

θ = jet impingement angle

ω = source term

Subscript,

tr = translational–rotational energy levels

ve = vibrational and electronic energy levels

s = species

CHAPTER 1

INTRODUCTION

1.1 Background

The design and analysis of effective thermal protection systems for hypersonic vehicles is a critical challenge in aerospace engineering. The leading edge of these vehicles are exposed to extreme heat flux due to the rapid stagnation of high enthalpy flow, making thermal management techniques necessary to maintain the structural integrity of the vehicle. Hypersonic maneuvering vehicles are usually designed with slender bodies and with sharp leading edges as shown in Figure 1. This configuration has the advantages of increasing vehicle maneuverability and increasing the lift to drag ratio. However, sharp leading edges will bring several design challenges, above all the issue of thermal management created by the small radius of curvature of the leading edge [1,2]. The numerical simulation is one of the best to evaluate the surface heat flux and other aerodynamic parameters compared to experiments and in-flight test [3,4]. Due to elevated temperature involved in the hypersonic flow, the molecular vibrational, rotational translational electronic energies are excited at different temperatures. The gas molecules dissociate and ionize due the elevated temperature. The gas molecules will undergo thermal and chemical non equilibrium. And it is critical to keep the temperature of the leading edge below the material melting point and below the thermal-structural limits. One way to control the temperature of the leading edge is by using an actively cooled Thermal Protection System (TPS). The active cooling of the TPS can be achieved using various methods such as film cooling, transpiration cooling, and impingement cooling [5]. The higher heat transfer of impingement cooling makes this method the widely used cooling techniques for hypersonic

leading. Impingement cooling involves injecting coolant through nozzles to impinge on the leading-edge surface. This cools the surface, reducing the heat loads and protecting the underlying structure. Impingement cooling can be further enhanced by using hybrid cooling methods, which combine film cooling and convective cooling to improve the thermal performance of the leading edge. In addition, it is easier to control the heat transfer rate by varying the geometry and position of the jets, and fluid flow parameters. Typical impingement coolant fluids are Hydrogen and Helium, which have been shown to have a poor cooling performance. [6]. Recently, it has been proposed to use Supercritical Carbon dioxide (sCO_2) as a cooling impingement liquid. In combination with the coolant, the overall cooling effectiveness depends also on other factors such as the structural materials, impingement geometry, and external flow conditions. The current study presents a systematic study to find the effect of jet impingement position angle (θ) and the jet position (H/d) on heat transfer for the provided operating conditions.

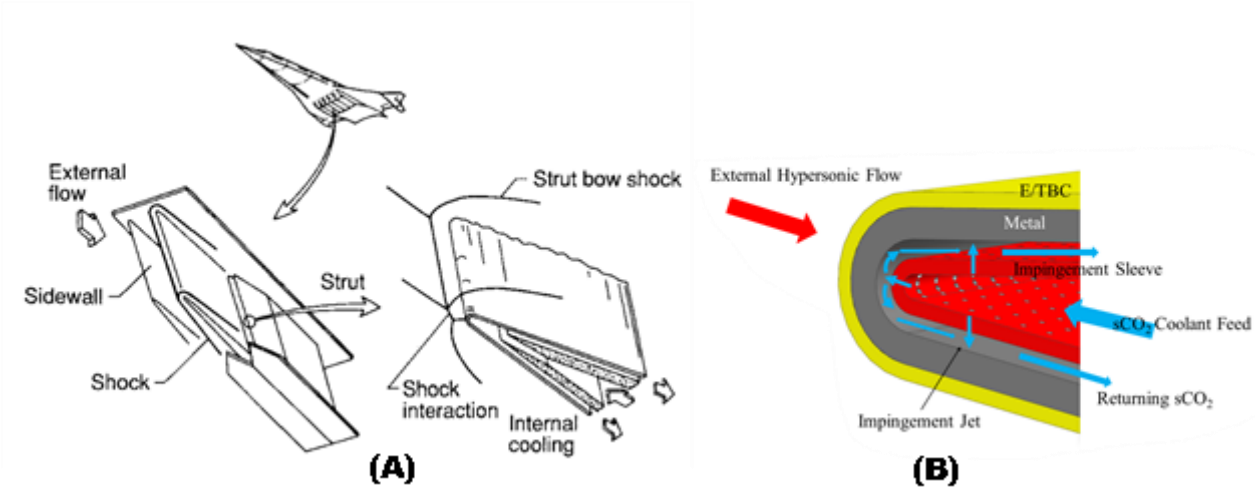

Figure 1 (a)Fluid-thermal-structural interactions on an aerospace plane scramjet engine leading edge[7] **(b) Schematic of two-layer (TBC and metal) leading-edge cooled with multiple sCO2 impingement jets.**

In addition, the current study extends the previous research done on the thermodynamic non-equilibrium hypersonic flow using the two-temperature model [8–11]. Less research has been done to combine the hypersonic flow with sCO_2 jet impingement cooling numerically [9,12]. In this study, an effort is taken to combine the non-equilibrium two temperature model with the gas model for the sCO2 region with multiple jet impingement. Also, the effect of using Supercritical CO_2 as the impinging coolant on high-temperature flows is unexplored.

.

This study aims to calculate the thermal performance of Supercritical CO_2 impingement cooling for various geometric configurations given in Table 1.

Table 1 Parameter range in the study.

Jet diameter (mm)	1
spacings between the nozzle exit and cooled surface (H/d)	1, 3, 5
Jet impingement angle θ	30^o, 45^o ,60^o
Jet Reynolds number	22,500

This study provides a comprehensive exploration of aero and heat transfer effects in hypersonic flows with sCO2 impingement cooling. The research combines numerical simulations and complex, yielding key findings.

1.2 The Problem Statement

The design and operation of hypersonic aerospace vehicles pose numerous intricate, multidisciplinary engineering challenges. Notably, the thermal management of leading edges, subjected to intense heat during flight, remains a major concern. Despite extensive research, there is currently no developed active impingement cooling technique using sCO2 that can effectively cool these structures under the highest aerodynamic surface heat fluxes.

This dissertation aims to address this critical issue by investigating an active impingement cooling system for hypersonic vehicles. The study focuses on a 3mm radius leading edge, utilizing supercritical carbon dioxide (sCO2) as the coolant. The research incorporates conjugate simulations that merge external hypersonic flow and sCO2 active cooling, using a thermodynamic non-equilibrium two-temperature model and various chemical models.

The objective of this dissertation is to contribute to the existing body of knowledge by providing a detailed analysis of active impingement cooling for hypersonic leading edges, integrating real gas effects and multiple chemical models. The study will investigate heat transfer enhancements through geometric variations and evaluate sCO2's potential as a coolant, addressing key facets of hypersonic vehicle thermal management. The goal is to develop a definitive solution for an aerospace plane-type leading edge and contribute to the development of a satisfactory cooling method.

Moreover, the dissertation explores the untapped potential of converting hypersonic vehicle heat flux to power using the sCO2 cycle. This aspect remains underexplored, representing a significant knowledge gap. Investigating this novel approach is crucial to understanding its feasibility and potential applications in the field.

1.3 Objectives

1. Numerical Model Validation: Validation of a numerical model for non-equilibrium flow over a nose cone is undertaken to demonstrate its suitability for hypersonic simulations.
2. Chemical Reaction Species Models: The impact of different models on heat flux and flow behavior in hypersonic environments is investigated, emphasizing the significance of chemical reactions.
3. Free-Stream Mach Number: The study reveals the influence of varying Mach numbers on temperature distribution and surface heat transfer, providing insights into heat transfer characteristics.
4. Thermal Barrier Coatings: The role of thermal barrier coatings, such as RCC, in reducing metal temperature and preventing melting is examined.
5. Jet Impingement: Analysis is conducted on jet impingement angles and distances (Z/D ratio), highlighting their significant influence on heat transfer enhancement.
6. Velocity Flow Field Analysis: Correlation between Nusselt numbers and flow velocity is established, offering insights for optimizing impingement angles and distances.
7. The study explores the potential of converting hypersonic vehicle heat flux to power using the sCO2 cycle. This novel approach could signify a significant progression in the field, harnessing power from aerodynamic heat flux.

1.4 Outline of the Thesis

Chapter 1: Introduction

In this chapter, the research problem is introduced, and the background of the topic is discussed. The aerodynamic heating problem in hypersonic vehicles and the importance of Thermal

Protection Systems (TPS) are discussed. The potential of using sCO2 as a coolant for TPS is also presented. The objectives and scope of the research are outlined.

Chapter 2: Literature Review

In this chapter, a comprehensive literature review on aerodynamic heating, hypersonic TPS, and sCO2 impingement cooling is presented. The most recent studies and the most relevant literature to the research topic are discussed.

Chapter 3: Numerical Methodology

In this chapter, the methodology used in the research is presented. The Ansys Fluent software is introduced, and the numerical simulation setup is discussed. The thermochemical nonequilibrium models of 5 species Park's model and 11 species Gupta's model are also introduced, and the simulation parameters are discussed.

Chapter 4: Results and Discussion

In this chapter, the results of the simulations are presented and discussed. The effects of sCO2 impingement cooling on the aerodynamics and heat transfer at the leading edge are analyzed. The results are compared between the 5 species Park's model and 11 species Gupta's model. The potential of using sCO2 as a coolant for the leading edge TPS is also discussed.

The fluid-solid coupled simulations are done with internal fluid sCO2 to test the capability of the numerical model in predicting the heat transfer performance. The results are discussed in terms of the effect of the relative coolant tube-to-leading-edge distance (H/D) and the impingement angles on the heat transfer performance.

Chapter 5: Heat To Power Conversion: Sc02 Cycle

This chapter explores the conversion of aerodynamic heating into electrical power using the sCO2 power cycle. It covers principles, efficiency, and applications, emphasizing the potential impact on sustainable energy solutions. The discussion includes key components, design considerations, and the latest advancements in the field, offering valuable insights for researchers and engineers.

Chapter 5: Conclusion and Future Work

In this chapter, the main conclusions of the research are presented. The potential of using sCO2 as a coolant for the leading edge TPS is discussed, and the capability of the numerical model in simulating the hypersonic flow with real gas effects is also discussed. The limitations of the research and the areas for future work are also outlined.

Chapter 6 Future work Recommendations

CHAPTER 2

LITERATURE REVIEW

2.1 Introduction

The chapter aims to introduce challenges associated with hypersonic flight and the role of impingement cooling. in managing of the dissertation's subject matter.

2.2 Hypersonic Flight and Thermal Challenges

The development of hypersonic vehicle cooling techniques has been a topic of interest for over six decades. Hypersonic vehicles are those that fly at speeds greater than Mach 5, and the aerodynamic phenomena that occur at these speeds are much more complex than those at lower speeds. The boundary layer, which is the gas layer near any solid surface where dissipative friction and heat transfer dominate, can grow quickly enough to have a significant impact on the entire flow-field. As a result, the development of hypersonic vehicle cooling techniques has been a critical area of research[13].

One of the earliest cooling techniques was the use of ablative materials[14], which would burn away as the vehicle re-entered the atmosphere, taking the heat with it. Later, researchers developed regenerative cooling, which involved circulating a coolant through channels in the vehicle’s structure to absorb heat. However, this technique was limited by the temperature of the coolant, which could not exceed the material’s melting point.[15,16]

In the 1960s, researchers began exploring the use of transpiration cooling, which involved injecting a coolant into the porous surface of the vehicle, where it would evaporate and carry

away heat. This technique was later combined with film cooling, which involved injecting a thin film of coolant onto the surface of the vehicle.[16–19]

Passive and active cooling are two techniques used in hypersonic vehicle leading edge cooling as shown in Figure 2 and Figure 3. While passive cooling involves the use of insulating materials to absorb heat, active cooling involves the use of a cooling system in the regions of highest heat flux near the leading edges and around the engine. [1]

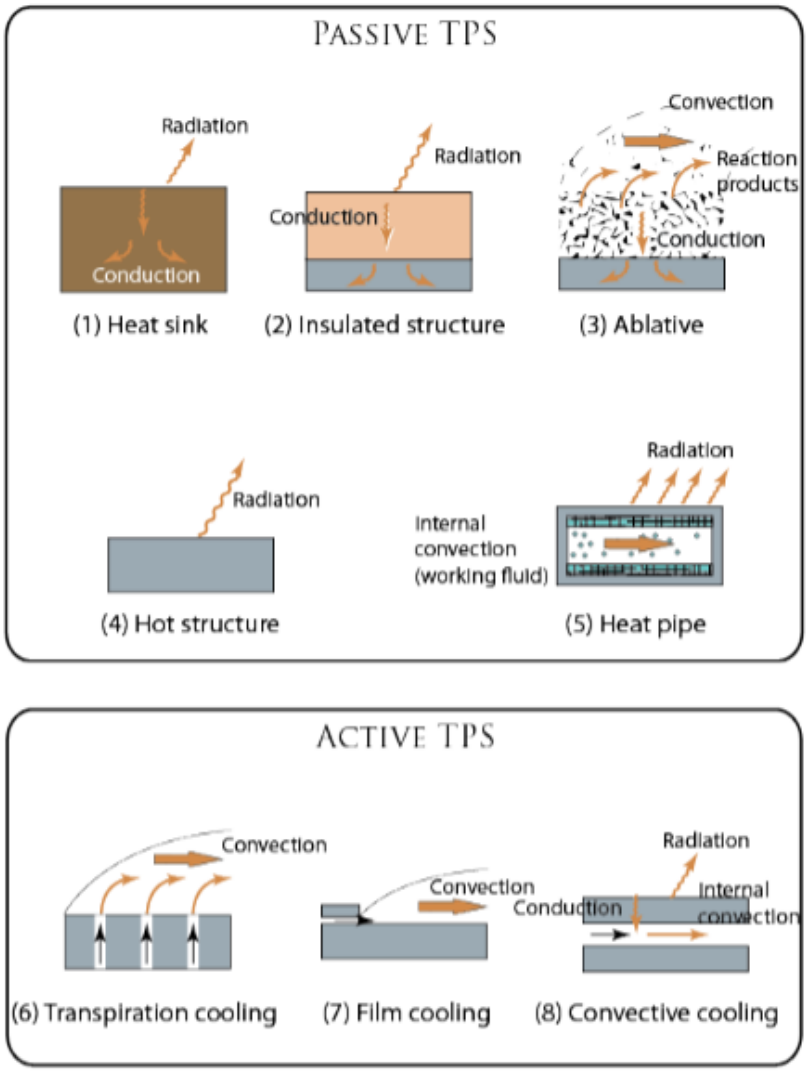

Figure 2 Thermal Protection concept of a Hypersonic vehicle.[1]

2.3 Cooling Techniques Used in Hypersonic Vehicle Leading Edge.

Hypersonic flight, characterized by speeds exceeding Mach 5, poses unique challenges in aerospace engineering. These challenges are primarily associated with the management of extreme temperatures resulting from air compression, which occurs as a hypersonic vehicle navigates through the Earth's atmosphere at high speeds.

As an object reaches hypersonic velocities, the collision of air molecules with its surface leads to intense heating known as aerodynamic heating or heat flux. This phenomenon is particularly pronounced at the leading edges of the vehicle, where the temperature increases rapidly.

The intensity of aerodynamic heating grows exponentially with increasing velocity, necessitating effective thermal management strategies to protect the vehicle and its occupants. Leading edges of hypersonic vehicles, exposed to extreme temperatures, require robust thermal protection systems.

2.3.1 Passive cooling technology

Key to managing thermal challenges in hypersonic flight is the selection of appropriate materials. Traditional aircraft materials are unsuitable for hypersonic conditions due to the extreme temperatures involved. Therefore, advanced materials with exceptional high-temperature resistance and ablative properties are utilized. These materials include ceramic composites, carbon-carbon composites, and refractory metals like tungsten.

Additionally, thermal barrier coatings (TBCs) are applied to the vehicle's surface to enhance its heat resistance. TBCs consist of multiple layers, including a bond coat and a ceramic layer. They function by insulating the vehicle's structure, creating a barrier between the extreme

temperatures and the underlying material. TBCs play a crucial role in extending the operational lifespan of hypersonic vehicles and ensuring their structural integrity.

The thermal challenges of hypersonic flight are closely intertwined with the structural integrity of the vehicle. The extreme temperatures experienced at the leading edges could cause material degradation and structural failure if not managed effectively. To address this, extensive testing and analysis are vital. The development of new materials and composites with enhanced thermal properties is also underway. These materials have the potential to withstand even higher temperatures and reduce the need for elaborate thermal protection systems.

2.3.2 Active cooling Techniques

Passive colling alone cannot cool the leading material in few flight conditions. So, Researchers and engineers are actively working on innovative solutions to tackle these challenges. One such innovation involves active cooling methods, such as impingement cooling. Impingement cooling systems use high-speed jets of coolant to dissipate heat from critical regions of the vehicle's surface, preventing overheating and contributing to more efficient flight.

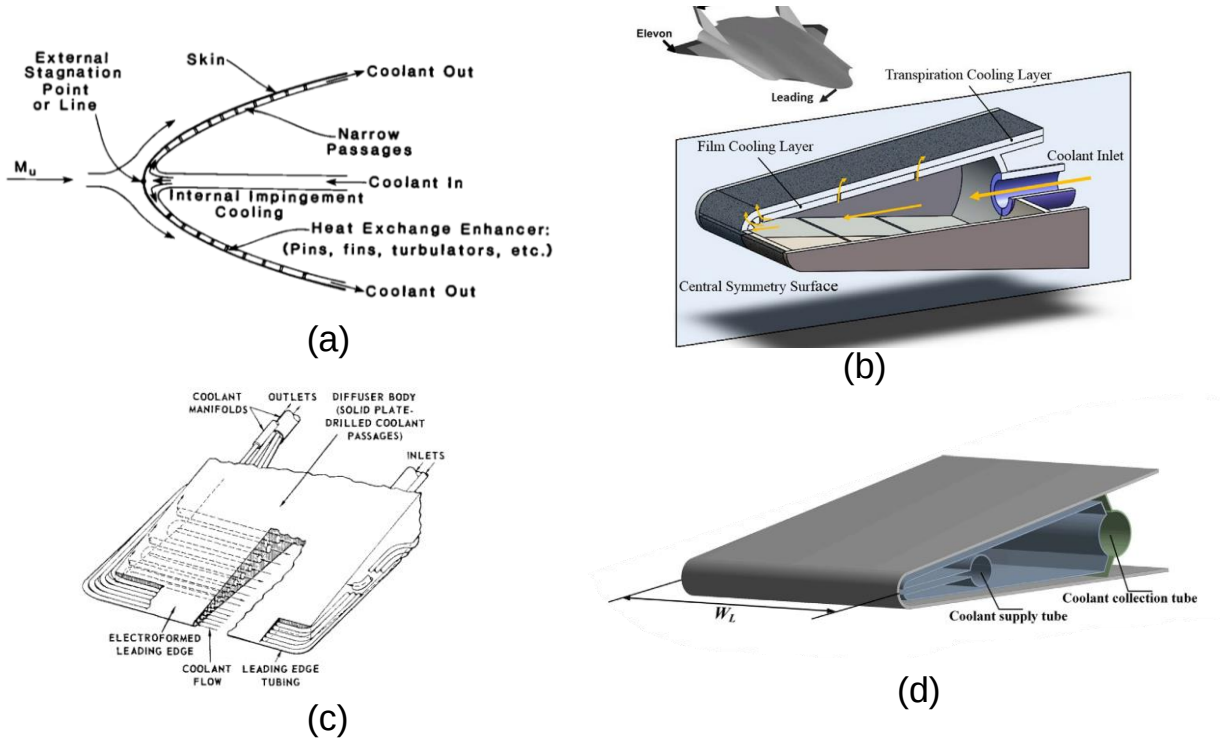

Figure 3 (a)Convection colling concept[20] **(b) transpiration cooled leading edge with Hydrogen**[16] **(c) water cooled leading edge**[21] **(d) helium impingement cooled leading edge**[6]**.**

Impingement cooling is a well-established thermal management technique utilized in various engineering applications, including the aerospace industry. It involves the directed flow of a cooling medium onto a heated surface to dissipate heat. In the context of hypersonic vehicles, impingement cooling plays a vital role in maintaining the structural integrity and performance of leading edges subjected to intense heat.

This comprehensive review[22] looks at impingement cooling over a variety of modifications and applications with a focus on improved manufacturing techniques impacting novel design and implementation. The primary mode of heat transfer enhancement is due to the flow stagnation. The effectiveness of jet impingement as a cooling technique is well documented; however, the application of jet impingement to different problems has been hindered by the

inability of manufacturing methods to incorporate impingement systems easily into cooling designs

In this innovative study proposed a unique double-layer cooling structure designed to tackle the formidable challenge of cooling the leading edge of hypersonic vehicles. The structure cleverly incorporated an outer porous layer and an inner layer utilizing nitrogen as a coolant. The research was a testament to the power of coupled numerical simulations, demonstrating their ability to optimize cooling techniques effectively.[23]

This study evaluates usage of Supercritical CO2 Impingement Cooling for a Hypersonic Leading Edge which offers simplicity and high heat transfer rates when compared to others, such as film cooling and transpiration cooling[9].

This research[24] introduces double layer transpiration cooling into the design of the cooling system in the leading edge of a hypersonic vehicle. The study considers effects of different kinds of coolants to reveal cooling mechanisms in different operation conditions. When different kinds of coolants supplied at the same mass flow rate, the coolants with low densities, i.e., H2 and He, have the lowest peak temperature compared with the coolants with large densities, i.e., N2 and CO2

An extensive investigation was conducted in this research, analyzing the heat transfer characteristics of jets impinging on concave surfaces under various annular and jet-to-surface distances. It culminated in the development of comprehensive correlations for heat transfer and flow characteristics.[25]

In a quest for cutting-edge cooling solutions, this study took a deep dive into the integration of heat pipes with high thermal conductance into hypersonic leading edges. It cleverly leveraged

finite element models and experimental data to showcase their effectiveness under high enthalpy conditions at Mach 7.[2]

Diving deep into the intricacies of fluid-thermal-structural analysis, this research examined various leading-edge concepts, deploying hydrogen as a coolant. The study convincingly demonstrated the effectiveness of impingement cooling in maintaining the leading edge's temperature within acceptable limits. Additionally, it shed light on the prospect of employing tungsten as a robust leading-edge material.[26]

In this meticulous study, the interaction between fluid and solid thermal aspects in cooling a hypersonic leading edge with hydrogen was scrutinized. It not only highlighted the cooling potential of hydrogen but also emphasized the ability of Multiphysics simulations to simulate hypersonic flow under diverse conditions. [27]

2.4 Thermal Barrier Coatings

Thermal barrier coatings are integral to hypersonic flight as they offer protection against extreme temperatures and thermal stresses. These coatings provide a shield against the harsh thermal environment, preventing structural damage. Understanding the materials and technologies behind thermal barrier coatings is essential for effective heat management in hypersonic vehicles. Thermal Barrier Coatings (TBCs) are a crucial component in hypersonic flow systems due to their ability to withstand extreme temperatures and thermal gradients. Here are some key findings from the literature:

Multifunctional Hypersonic Components and Structures: A team at Johns Hopkins University Applied Physics Laboratory (APL) conducted a strategic independent research and development project exploring multifunctional hypersonic components and structures1. APL

developed transformational materials technologies and expertise that could be applied to relevant hypersonic vehicle programs supported at APL. The team identified several areas of concentration to support the needed hypersonic materials science and technology and engineering. One of the most challenging areas for these vehicles is the vehicle leading edge and control surface leading edges[28].

Mechanical Integrity of Thermal Barrier Coatings: A coating system was designed for a generic engine to demonstrate the benefits of TBCs in rocket engines. The coatings were tested in a hypersonic wind tunnel with surface temperatures of 1350 K and above, where no coating failure was observed[29].

Thirty Years of Thermal Barrier Coatings (TBC), Photothermal: This work summarizes the research and the development of techniques specifically aimed at measuring the thermophysical properties, the characterization of the microstructure and the identification of adhesion defects to the metal component of the TBCs[30].

Thermal Barrier Coatings for High temperature materials: The literature review involved the detailed investigation of thermal barrier coatings applied on nickel-based superalloys with particular emphasis on their high-temperature performance (mechanical response and oxidation resistance)[31].

2.5 Numerical Simulations and Modeling

Wind tunnel testing is a common approach used to simulate hypersonic conditions and evaluate the performance of materials and thermal protection systems. Test articles are exposed to high-velocity air flows in wind tunnels, replicating the aerodynamic heating and thermal stresses they would experience in actual flight. These tests provide essential data for material selection

and TBC design. However, conducting hypersonic wind tunnel experiments is expensive and challenging to set up. Nowadays, numerical simulations are employed for a quick and effective solution.

Numerical simulations, such as Computational Fluid Dynamics (CFD) and Finite Element Analysis (FEA), are also employed to model the behavior of hypersonic vehicles. These simulations allow engineers to study the effects of aerodynamic heating and assess the thermal and structural response of the vehicle. By understanding the thermal challenges through simulations, researchers can fine-tune the design and heat management strategies.

Mathematical models are instrumental in simulating and predicting the behavior of impingement cooling in hypersonic flow. This section explores the various models and numerical techniques used to study heat transfer, aerodynamics, and fluid dynamics, shedding light on the role of numerical simulations in advancing our understanding. Below are some of the literary works that explore non-equilibrium thermodynamic models and hypersonic conjugates simulations.

In this comprehensive study, a 3-inch diameter leading edge was subjected to testing at a Mach number of 6.47. The research harnessed the finite element method to delve into the integrated fluid-thermal structure of the leading edge. It not only highlighted the potential of an integrated approach for solving hypersonic leading-edge challenges but also provided crucial insights into the thermal-structural response and complex interactions.[7]

This research embarked on a numerical journey, employing various air species models (including 5 species, 7 species, 11 species, and Gupta's model) to simulate flows over a sphere.

Notably, it identified a seven-species model as suitable for high Mach numbers in hypersonic flows.[32,33]

This study[34] vigorously validated the practicality of using two-temperature models to simulate flows over a double cone. The findings highlighted the consistency in results achieved through this approach, underpinning its reliability in numerical simulations.

Delving into high enthalpy flows over a double cone, this study compared the outcomes of employing various models, including the Park species model, and coupled vibration dissociation vibration (CVDV) model. It also illuminated the disparities between experimental data and numerical models, paving the way for further refinement.[35,36]

This study ventured into the realm of hypersonic flow over a cone in a shock tube, leveraging non-equilibrium models. Importantly, it demonstrated the capacity of numerical simulations to reasonably predict surface pressure measurements, heat flux, standoff distance, and emulate experimental measurements.[4]

In the context of high-temperature hypersonic vehicles, this paper delved into the complexities of rate effects. It explored gas-phase reactions and non-equilibrium thermal-chemical states, shedding light on the intricacies of these phenomena.[37]

This paper cast a discerning eye on computational fluid dynamics (CFD) modeling, emphasizing viscous wall boundary conditions, multi-zone coupling for fluid-thermal interaction, and cross-scale algorithms. It dissected the modeling methods related to interface effects and their corresponding coupling algorithms. [38]

This study embarked on the audacious mission of assessing the practicality of applying theoretical and empirical models for vibrational relaxation, dissociation rates, and vibration-rotation coupling effects on numerical simulations, offering fresh insights into the topic.

It undertook a meticulous examination of various thermo-chemical non-equilibrium models, such as Park's five species and Gupta's 11 species models, to simulate hypersonic flows. The study dissected the effects of ionization and wall catalysis, offering valuable insights into the complex interplay of these factors.[39]

This study brought ANSYS Fluent into the equation, scrutinizing the modeling of cylinder reentry spacecraft using Park's five species and Gupta's models. It painted a picture of reasonable agreement between the models and experimental data, underlining the potential of these models in numerical simulations.[11,40]

2.6 Emerging Trends in Hypersonic Leading-Edge Cooling

Advancements in materials and technologies are continually shaping the field of hypersonic leading-edge cooling. Recent research has unveiled innovative approaches and promising materials to enhance the efficiency and effectiveness of cooling systems. This section discusses emerging trends and future directions in the domain of hypersonic cooling.

In a quest for cutting-edge cooling solutions, this study took a deep dive into the integration of heat pipes with high thermal conductance into hypersonic leading edges. It cleverly leveraged finite element models and experimental data to showcase their effectiveness under high enthalpy conditions at Mach 7.[2]

In a bold exploration of leading-edge materials, this study unveiled the potential of metallic lattice frame structures when exposed to hypersonic conditions. Researchers meticulously examined their heat transfer performance and thermal-structural responses. The findings offered strong evidence of the viability of these structures in handling high heat flux conditions characteristic of hypersonic flows.[41]

In this forward-thinking study, the possibility of incorporating heat pipes into the structure of hypersonic leading edges was explored. It scrutinized the thermal boundary conditions and introduced the innovative use of lithium as a working fluid to cool the leading edge in the Mach number range of 6 to 8.[42]

2.7 Gaps and Research Questions

1. **Validation of Numerical Model:**

   How well does the chosen numerical model perform in simulating non-equilibrium flow over a hypersonic nose cone, and what is the agreement between numerical simulations and experimental data?

2. **Influence of Chemical Reaction Species Model:**

   What is the impact of different chemical reaction species models on heat flux and flow behavior in hypersonic flow, specifically comparing the 11-species Gupta's model and the 5-species Park's model?

3. **Effect of Free-Stream Mach Number:**

How does varying the free-stream Mach number affect the temperature distribution and surface heat transfer coefficient at the leading edge in hypersonic flow scenarios?

4. **Influence of Thermal Barrier Coatings:**

   How do thermal barrier coatings, like Reinforced Carbon-Carbon (RCC), affect the metal temperature and overall temperature of the leading edge in hypersonic flow?

5. **Jet Impingement Angle and Distance (Z/D ratio):**

   What is the impact of jet impingement angle and the distance between impingement points (Z/D ratio) on heat transfer, and how does the choice of Z/D ratio influence heat transfer enhancement?

6. **Velocity Flow Field Analysis:**

   How does the velocity flow field analysis explain the observed trends in Nusselt numbers, and what is the relationship between Nusselt numbers and the velocity of the flow field?

7. **Effect of Impingement Jets:**

   What is the effect of impingement jets on cooling solid metal surfaces, and how does cooling with impingement jets reduce the temperature on the solid surface compared to cases without cooling?

.

CHAPTER 3

NUMERICAL METHODOLOGY

A hypersonic flow field undergoes thermochemical nonequilibrium due to elevated temperature after the shock layer. The complexity of the hypersonic reentry flows makes the ground testing experiments in wind tunnels and shock tunnels harder. It is difficult to obtain necessary data from experiments such as surface oxidation, heat transfer coefficient, etc., The free stream flow conditions are chosen to be within the continuum range.

In a hypersonic flow, the integral energies of the molecules cannot be repressed in a single temperature. The vibration energy levels affect dissociation and affect the vibrational energy of the molecules due to elevated temperature. The vibration dissociation coupling is considered by the two temperature conditions. In Two temperature conditions, the transitional and rotational energy is considered in equilibrium with one temperature. The vibrational and electronic temperatures are in equilibrium with the second temperature (i.e., $T_{tr} \neq T_{ve}$). In this study, Ansys fluent 2022R2 version is used to solve the flow field [43,44]. Also, Fluent numerical simulations are widely used in high-speed flows to predict the properties that are difficult to extract from the experiments [9,45–50]. The simulation uses the multi-species compressible Navier stokes equation in the continuum regime [43,44].

3.1 Conservation Equations

The dissertation employs the ANSYS FLUENT Workbench as the comprehensive solver, covering tasks from geometry creation to post-processing. The simulation setup adopts an axis-symmetric configuration with double precision (dp) and utilizes a steady-state Density-Based

Navier-Stokes (DBNS) solver. The numerical scheme incorporates Green-Gauss Node-Based gradient for viscous fluxes and the AUSM scheme. Turbulence modeling is implemented through the Reynolds-Averaged Navier-Stokes (RANS) approach, specifically utilizing the Two-equation Shear Stress Transport (SST) k-ω model. The working fluids considered are air species for external flow and supercritical carbon dioxide (sCO2) for internal flow. Species modeling follows a species-species approach for both internal and external flow fields. For internal flow, the air-5species-park93 model represents a mixture of N2, O2, NO, N, and O, employing Park 93 chemical mechanisms, while the air-11species-gupta model includes N2, O2, NO, N, O, N2+, O2+, NO+, N+, O+, and e-, using Gupta chemical mechanisms. The finite-rate chemistry solver is employed, incorporating direct source terms. Thermochemistry simulations are conducted with a Two-Temperature (2T) non-equilibrium approach to accurately represent the flow conditions. The models assume that the air consists of five species for Park 5-species and 11 species for Gupta's 11 species, and that the translational-rotational and vibrational modes of the molecules have different temperatures (i.e., $T_{tr} \neq T_{ve}$). The conservation equations for mass, momentum, energy, and species are the same as in the park 5-species model, except for the net production rate of each species. The net production rate of each species is calculated by summing up the contributions of all the reactions that involve that species. The model accounts for the effects of ionization, dissociation, recombination, and chemical reactions among the species, as well as the Joule heating due to the electric field.

The model consists of the following equations:

The continuity equation for each species:

$$\frac{\partial \rho_i}{\partial t} + \nabla \cdot (\rho_i \boldsymbol{u}) = \boldsymbol{Wi} \quad (1)$$

where ρ_i is the density of species i, u is the velocity vector, and Wi is the net production rate of species i due to chemical reactions.

The momentum equation of the Park's 5-species and Gupta's 11-species model is the same as the general conservation equation for momentum in a fluid.

$$\frac{\partial}{\partial t}(\rho \boldsymbol{u_i}) + \nabla \cdot (\rho \boldsymbol{u_i u}) = -\frac{\partial p}{\partial x_i} + \nabla \cdot \boldsymbol{\tau_{ij}} \quad (2)$$

where ρ is the density, u_i is the i-th component of the velocity vector, p is the pressure, and τ_{ij} is the viscous stress tensor. The difference between the Park 5-species and Gupta 11-species models lies in how they calculate the pressure and the viscous stress tensor, which depend on the thermodynamic properties, transport properties, chemical kinetics, and energy relaxation processes of the gas mixture [51] [52] [53,54]

The energy equation for each mode:

$$\rho \frac{De_{tr}}{D_t} = -p\nabla \cdot \boldsymbol{u} + \nabla \cdot (\boldsymbol{k_{tr}} \nabla \boldsymbol{T_{tr}}) + \boldsymbol{Q_{J,tr}} + \boldsymbol{Q_{R,tr}} \quad (3)$$

$$\rho \frac{De_v}{D_t} = -p\nabla \cdot \boldsymbol{u} + \nabla \cdot (\boldsymbol{k_v} \nabla \boldsymbol{T_v}) + \boldsymbol{Q_{J,v}}, + \boldsymbol{Q_{R,v}} \quad (4)$$

The source term $\boldsymbol{Q_{J,v}}$ in Equation 4 models the relaxation between translational and vibrational modes. The relaxation source term is modeled using the Landau-Teller theory as

$$\boldsymbol{Q_{J,v}} = -\frac{\langle E_v \rangle - \langle E_v \rangle_0}{\tau}$$

where ⟨Ev⟩ is the average vibrational energy, ⟨Ev⟩0 is the equilibrium value, and τ is the relaxation time. The relaxation time depends on the temperature and the vibrational state-to-state rate coefficients.

where e_{tr} and e_{ev} are the translational-rotational and vibrational energies per unit mass, $k_{tr}$and k_v are the thermal conductivities for each mode, T_{tr} and T_v are the translational-rotational and vibrational temperatures, and $Q_{J,tr}$, $Q_{J,v}$, $Q_{R,tr}$, and $Q_{R,v}$ are the source terms due to Joule heating and chemical reactions for each mode.

The model requires additional equations for the electric potential and current density, as well as appropriate boundary conditions and initial conditions. The model also requires thermodynamic and transport properties of the air species, such as specific heats, enthalpies, internal energies, electrical conductivities, viscosities, diffusion coefficients, reaction rates, etc. $Q_{J,tr}$, $Q_{J,v}$, will become zero in the equations for non-equilibrium hypersonic flow without considering the effects of ionization and recombination.

The main difference between the reactions considered in the Park 5-species model and the Gupta 11-species model is that the Gupta 11-species model includes the ionization reactions of air molecules, while the Park 5-species model does not. Ionization reactions are important for hypersonic flows at very high temperatures and altitudes, where the air molecules can become partially or fully ionized. The Gupta 11-species model considers 11 species: N2, O2, NO, N,

O, N2+, O2+, NO+, N+, O+, and e-. The Park 5-species model considers only five species: N2, O2, NO, N, and O. The reactions considered in both models are:

$$\begin{array}{rcl} \text{Dissociation:} & N_2 + M & \rightleftharpoons N + N + M \\ & O_2 + M & \rightleftharpoons O + O + M \\ \text{Recombination:} & N + N + M & \rightleftharpoons N_2 + M \\ & O + O + M & \rightleftharpoons O_2 + M \\ \text{Exchange:} & N_2 + O & \rightleftharpoons NO + N \\ & O_2 + N & \rightleftharpoons NO + O \end{array}$$

where M is any heavy particle (N2, O2, NO, N, or O). The additional reactions considered in the Gupta 11-species model are:

$$\begin{array}{rcl} \text{Ionization:} & N_2 + M & \rightleftharpoons N_2^+ + e^- + M \\ & O_2 + M & \rightleftharpoons O_2^+ + e^- + M \\ & NO + M & \rightleftharpoons NO^+ + e^- + M \\ & N + M & \rightleftharpoons N^+ + e^- + M \\ & O + M & \rightleftharpoons O^+ + e^- + M \end{array}$$

where e^- is an electron. These reactions affect the thermodynamic properties, transport properties, chemical kinetics, and energy relaxation processes of the gas mixture. More details about the thermo-non equilibrium and chemical reaction models can be found elsewhere in the literature [37,54,55].

The pressure of the species is calculated by the mixture of partial pressures.

$$\boldsymbol{p = \sum_{s=1}^{ns} p_s = \sum_{s \neq e-} \frac{\rho_s R_u T}{M_s} + \frac{\rho_e R_u T_e}{M_s}} \qquad \textbf{(5)}$$

Internal energy per unit mass consists of vibrational, rotational, electronic, and chemical energy of the species.

$$\mathbf{Es = Et_{rs} + E_{rots} + E_{vs} + E_{es} + \Delta h_s}$$

(6)

The Cp values are obtained by NASA (National Aeronautics and Space Administration) polynomial, and it is considered as piecewise linear for all species. The ideal gas mixing law is used to find the thermal conductivity and viscosity of the gas. A coupled flow simulation is conducted by combining the external air region and solid region with multiple internal sCo2 jets. The simulation of external nonequilibrium aerodynamics with impingement cooling is an attempt to capture the thermal performance of the sCo2-cooled leading edge. This numerical method is validated by the experimental results as shown in Figure 12[4]. To simulate the conjugate simulation, the specific model is used in the internal and external stimulation. The species-species model approach is followed to model the internal and external flow fields. In the external flow, the mass fraction of carbon dioxide is taken as zero and oxygen as 0.23, and nitrogen as 0.77. But in the internal flow region carbon oxide mass fraction is taken as 1 ignoring all other species. It makes sure that, in the internal region carbon dioxide is kept as coolant. Simulation boundary conditions are shown in Figure 6. Conjugate heat transfer is considered for the simulations. The internal side of the solid is coupled to the sCO2 fluid domain. It is expected that the hole-specific jet Reynolds number will be varying along with the array as only the overall sCO2 feed conditions are fixed. The hole-specific mass flow rate is determined by geometry. The model has a 0.25 mm (about 0.01 in) radius nose cone, 0.05mm thickness of the pure tungsten metal region,0.05 mm thickness of carbon reinforced matrix. The thermophysical properties, including the melting points, of Thermal Barrier Coating Composite (Carbon Fiber-Reinforced Carbon Matrix) and Metal Tungsten Pure Alloy is provide in that Table 2.

Table 2 Thermo-Physical properties of the Solid and TBC

Material Property	**Density (ρs) (kg/m³)**	**Specific Heat (cPs) (J/kg K)**	**Thermal Conductivity (ks) (W/m K)**	**Melting Point (°C)**
Carbon Fiber-Reinforced Carbon Matrix	1699.9	756	26.268	~3000
Metal Tungsten Pure Alloy	19300	129.12	172.4	3422

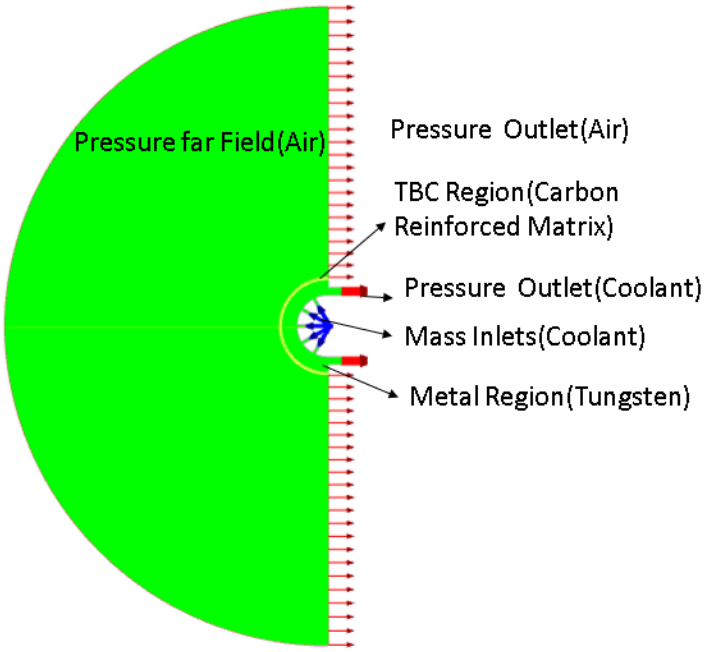

Figure 4 Numerical setup.

3.2 Meshing Details

To capture the complex flow field, the flow field mesh is made from structured elements using Ansys Mesher. The grids near the wall are refined to capture shock waves and boundary layers, and y+ values near the wall are maintained at less than 1. Mesh quality is maintained between 0.9 to 1. Grid-independence studies are conducted with four different grids from coarser to fine. The mesh independent study helps to capture the variations due to the mesh refinement. The pressure predicted by all four mesh girds is plotted as shown in Figure 5. The finer mesh with 114885 and 51520 cells shows no variation in the pressure along the axis. The fine mesh with the cell counts 51520 is used for further study. The configuration involves four interconnected domains, comprising two fluid domains (Air and CO2) and two solid domains

(TBC and Metal). These domains are linked through three interfaces to establish a comprehensive system for analysis.

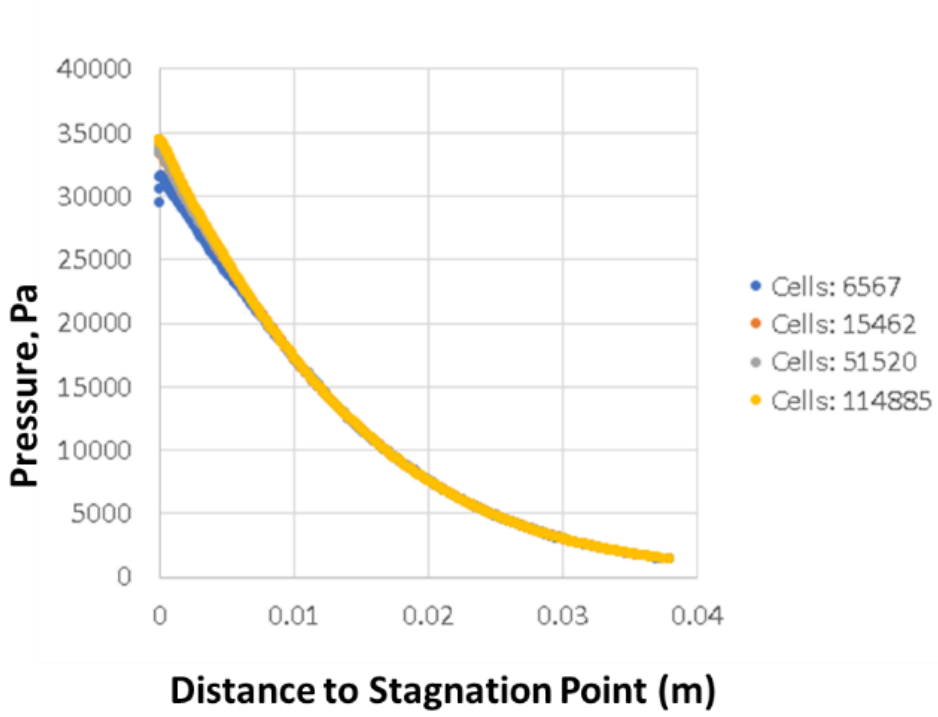

Figure 5 Grid independence study

3.3 External Flow Methodology Validation

The methodology presented in the previous section is validated using the experiments conducted by MacLean et al[3]. The free stream conditions for these experiments are as follows:

- Mach number: 12.4
- Free stream pressure: 215.31 Pa

- Temperature: 296 K
- Reynolds number: 0.45 million/m
- Density: 0.002497 kg/m³

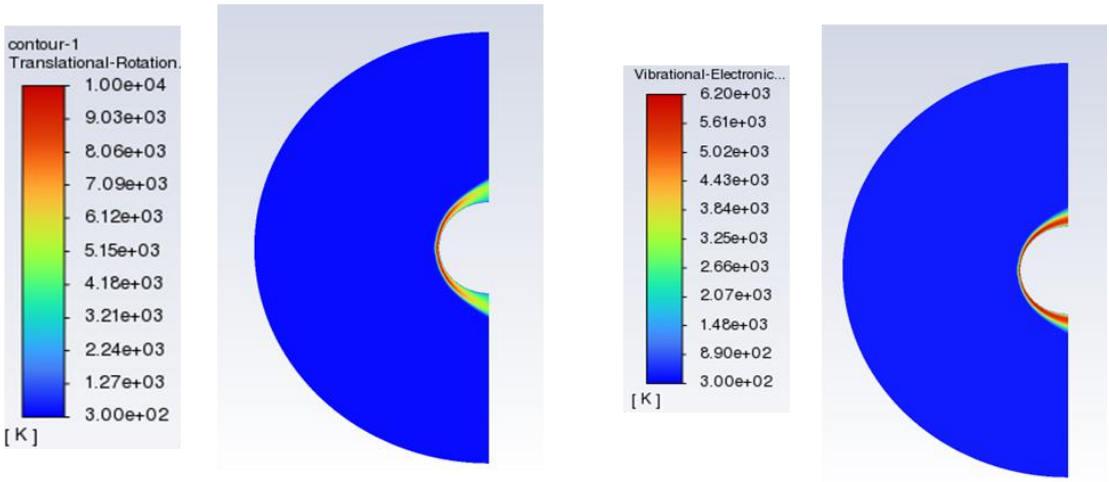

Figure 6 Contours of Translational and Electronic Temperature in the non-equilibrium Region

The simplified domain closely aligns with a current model case chosen from the literature by MacLean et al[3]. The model is simulated for the free stream conditions of Mach number 12, as provided in run 68 of the publication. The free-stream conditions fall well within the non-equilibrium conditions. The non-equilibrium flows are maintained such that air can exist in two states. The contributions of the translational and electronic temperatures are depicted as contours in Figure 6.

The grids are generated using the Ansys Mesher, with the geometry created inside Ansys Design Modeler. Three 2D grids are generated with cell counts of 114885 (Grid 1), 51552 (Grid 2), and 15,462 (Grid 3). The results from these grids are plotted in Figure 7. It is demonstrated that the grid with 51552 cells offers the best combination of accuracy and computational efficiency. While the solution on grid 2 is not fully grid-converged, its accuracy

is deemed sufficient to capture the key physical trends. Consequently, the grid with 51552 cells is selected for further studies.

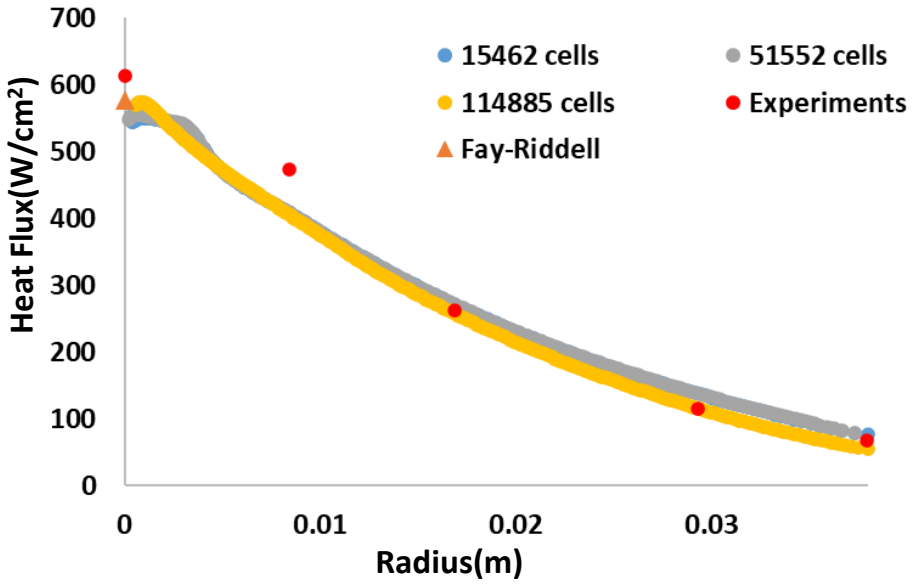

Figure 7 Results of Grid Convergence Study

In Figure 7, the pressure values obtained from the three different grids are plotted. It is evident that the property values do not change with the different grid nodes. The grids are refined near the impingement wall and the boundary layer. The y+ values are kept below one for all the simulations.

The surface heat flux, a critical parameter affecting the leading edge of the wing, is compared against the numerically simulated results as shown in Figure 7. The stagnation points heat flux, calculated from the Fay-Riddel model for the free-stream Mach number, is 577.40 W/cm². The calculated heat flux is comparable to the heat flux calculated in the simulations, which are located at 38 mm in Figure 7.

3.4 Enhancing Simulation Accuracy Through Temperature-Dependent Properties: A Case Study with Tungsten Material in Hypersonic Conditions

The material properties undergo changes based on temperature, particularly at higher temperatures. The variation in specific heat and thermal conductivity of tungsten is illustrated in the Figure 8, highlighting the necessity of implementing temperature-dependent properties in the simulations. Systematic examination of the thermal-dependent properties of the metal within the simulation was conducted. Simulations for the base case were executed with a Mach number of 7, utilizing tungsten as the material. To improve simulation accuracy, temperature-dependent properties derived from polynomials specific to tungsten, as referenced in authoritative texts on Tungsten metallurgy, were incorporated. A detailed comparative analysis of the recalculated results is attached for your reference.

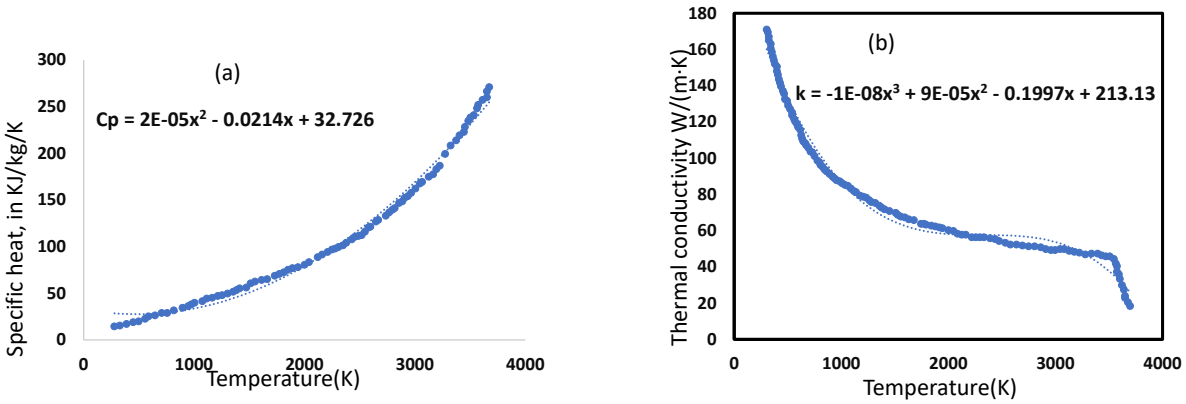

Figure 8 Temperature dependent thermophysical properties of tungsten, thermal conductivity, and heat capacity[56,57]

In further calculations, the constant temperature of the metal is utilized at lower Mach number conditions, such as Mach 7. However, it is imperative to implement temperature-dependent properties for other Mach number conditions or in higher temperature regions.

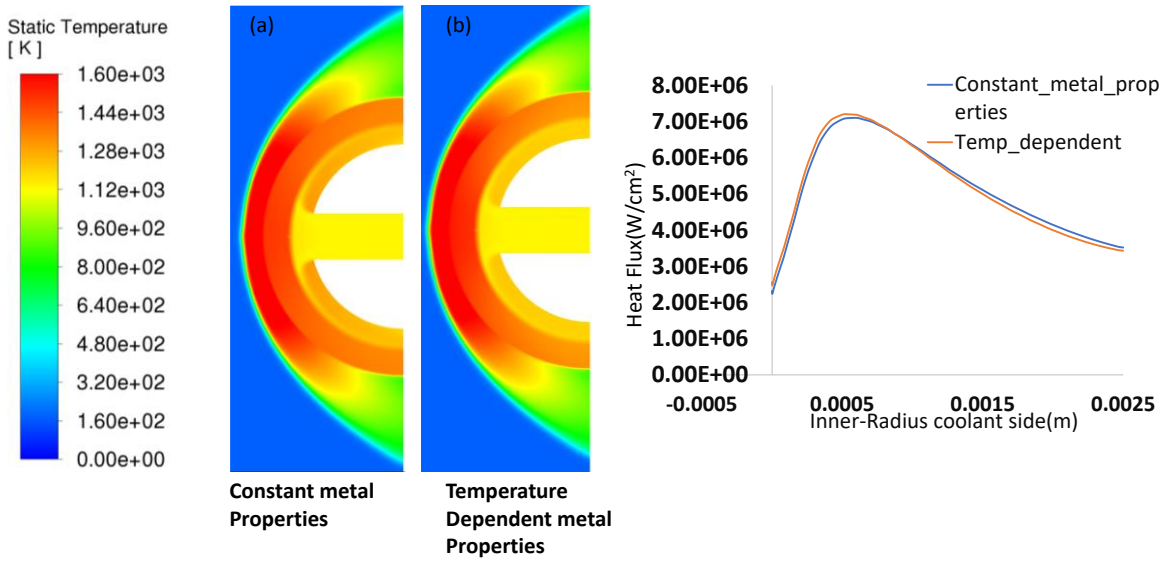

Figure 9 Temperature and Heat Variations Influenced by Material Temperature Dependency

Upon Investigation, it is notable that the disparities between simulations featuring temperature-dependent properties and those employing temperature-independent properties are minimal as shown in Figure 9 . This suggests that the inclusion of temperature-dependent properties, derived from comprehensive references, introduces marginal variations to both constant metal properties and heat flux in the simulated scenarios.

3.5 Internal Flow sCO_2 Jet Impingement Validation

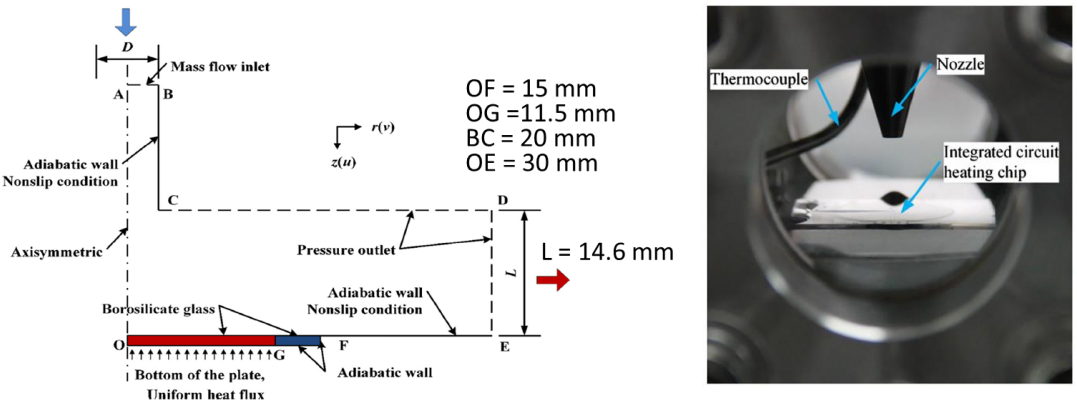

Figure 10 Validation Experimental Setup of the imping sCO_2 jet[58]

Simulations are conducted to investigate the fundamental fluid dynamics and heat transfer effects of sCO2 impingement cooling. The initial computational setup replicates a heated wall without external hypersonic flow, following the methodology outlined in Chen et al.'s experimental study[58,59]. Specifically addressing the heated leading edge, heat flux data from Table 1 is incorporated due to the limited literature on sCO2 impingement conjugate simulations. The simulations commence with sCO2 impingement for comparative purposes, enabling subsequent comparisons against air results and existing sCO2 impingement findings. NIST tables are employed for simulation accuracy, and Figure 12 exhibits satisfactory agreement between experimental data and the current simulations. The validation setup, modeled after the paper[60] is presented in Figure 10

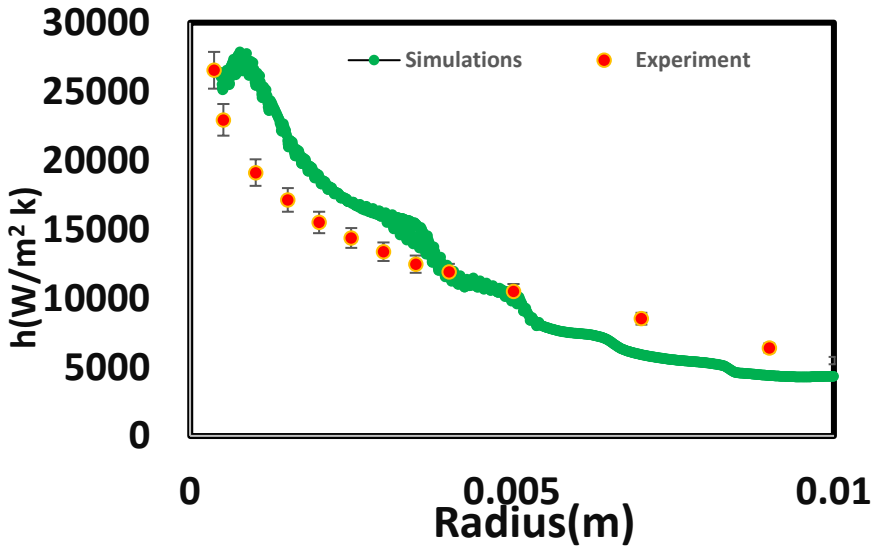

Figure 11 Comparison of the local heat transfer coefficient predictions (m = 22.36 kg/h, 0.22 MW/m2, p = 7.85 MPa, Tin = 18.0[58]

CHAPTER 4

RESULTS AND DISCUSSION

Numerical simulations are done to study the basic aero and heat transfer effects of sCO2 impingement cooling. A numerical test setup is created as shown in Figure 4 combining external hypersonic flow with impingement cooling. The test setup has two regions, one consisting of air and another region consisting of Supercritical carbon dioxide. The leading-edge solid region has two layers of one-layer Thermal Barrier Coating made of Carbon reinforce matrix and the metal layer is made of tungsten. The non-equilibrium Ansys fluent solver is used to solve the external hypersonic flow region and sC02 Ideal gas model is used to solve the sC02 region.

4.1 Ansys Fluent Code Validation for A Non-Equilibrium Flow Over a Nose Cone.

In hypersonic flow, the air undergoes disassociation. It means, that air internal energy modes-rotational, vibrational, translation, electronic, and so forth will reach equilibrium with new energy states at different temperatures. The air at hypersonic speed will not be characterized by a single temperature. The thermodynamic non-equilibrium two-temperature 5 species park's model in Ansys Fluent is used to simulate the flow field. The possibility of using the model in hypersonic flow is validated by the hypersonic flow experiments at a Mach number of 9.73. The numerical is done to test the viability of the Nonequilibrium model as compared to the Equilibrium model.

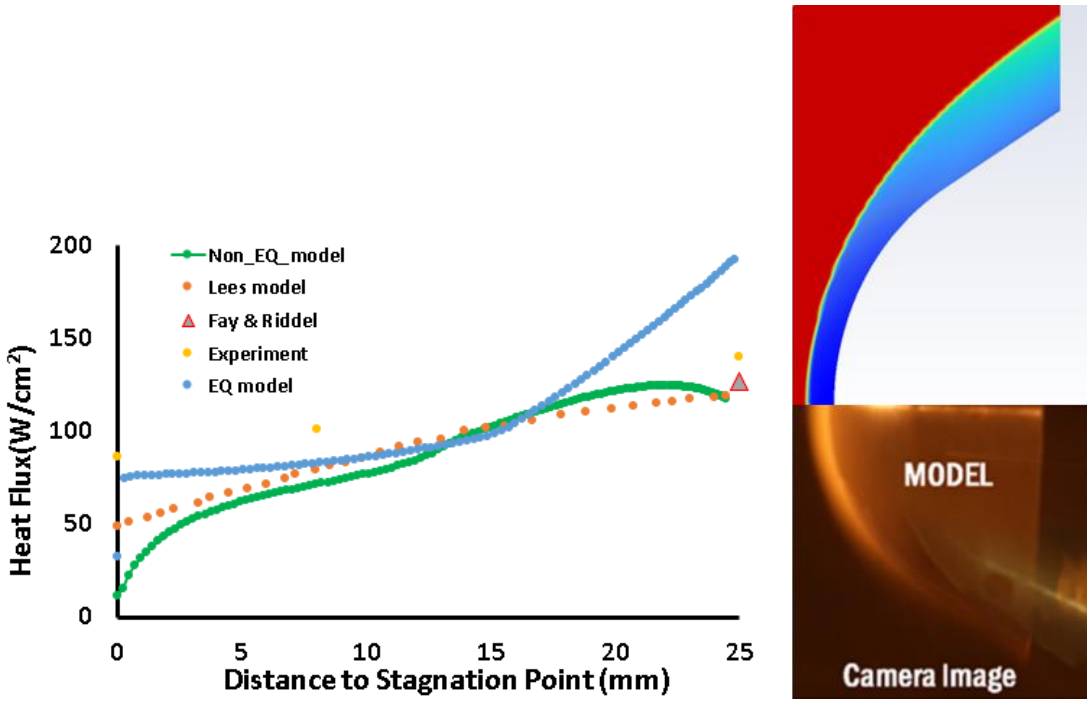

Figure 12 Heat flux and Flow field comparisons between experiments and simulation

The results shown in Figure 12 explains plotted to compare the heat flux and image visualization from experiments [4]. It is observed that the two-temperature models are predicting the heat flux over the nose cone well compared to the equilibrium model. Small discrepancies are observed between the experiments and numerical simulation due to the nonavailability of non-equilibrium experimental conditions. The results are compared with the theoretical equation [20,21] as shown in Figure 12. The reason behind the two-temperature models performs better in predicting heat flux over the nose cone compared to the equilibrium model is rooted in their ability to capture the dynamic nature of hypersonic flow. In hypersonic conditions, the air molecules undergo dissociation, and they exhibit various internal energy modes, each with its unique temperature. This dynamic equilibrium among these modes has a substantial impact on heat transfer and the overall behavior of the flow.

The two-temperature models account for this non-equilibrium state by considering separate temperatures for translational and vibrational energy modes. These modes are particularly important in hypersonic flow. This additional level of detail allows the model to make more accurate predictions about how heat is distributed over the nose cone. In contrast, the equilibrium model simplifies things by assuming a single, uniform temperature for the entire flow.

The enhanced accuracy of the two-temperature models in predicting heat flux underscores their ability to represent the complex interactions of energy modes in hypersonic air. This enables them to provide a more realistic and comprehensive description of the physical processes at work in hypersonic flow.

4.2 Effects Of Chemical Reaction Species Model

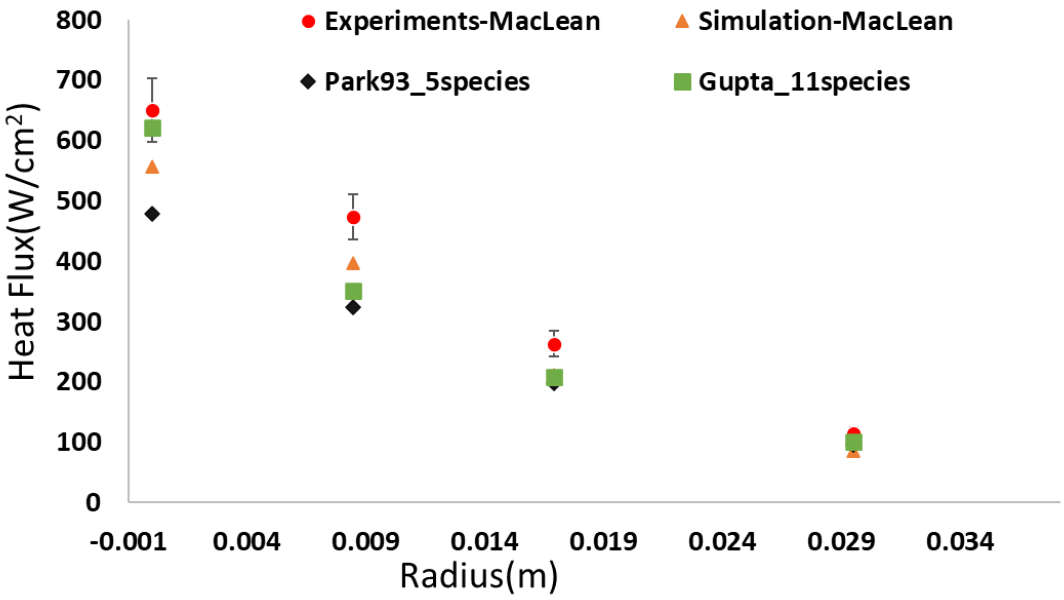

Figure 13 Heat flux comparison of two distinct species model

Numerical simulations are done to study the effect of changing the chemical reaction species model on the heat flux. The experimental values are taken from the LENS-XX expansion tunnel at CUBRC with the free stream conditions of Mach number 12 as provided in run 68[3]. In this study, Gupta's 11-species model, and the park is 5 species 93 model chemical reaction models are used to simulate the hypersonic flow. Figure 13 shows the simulated heat flux for the nose cone from two different species models compared with the experimental values and simulated values from the literature. The 11 species of Gupta's model predict a higher value of the heat flux compared to the 5 species model. But the heat flux predicted by both Park's model and Gupta's model does have a minor difference between the heat flux values. This is explained with the help of Figure 14 shows the vibrational-electronic temperature and translational-rotational temperature contours comparison between the two models. The 11-species predicts a higher temperature as compared to the 5-species model. As we all know, chemical reactions will increase the temperature of the gases. Since the 11 species model has 6 more species as compared to the 5 species model. The extra 6 species will go through more chemical reactions than the 5. This can be seen in the increase in temperature flow fields and heat flux.

The nitrogen and oxygen species, O, N and NO mass fractions predicted by both models are same in most of the region. But near the stagnation the mass fractions values of all the species slightly vary between the models. This shows that the difference in chemical reaction between both models is larger near the stagnation region. however, variations in mass fractions are evident near the stagnation region, emphasizing differences in chemical reactions, which likely contribute to variations in heat flux.

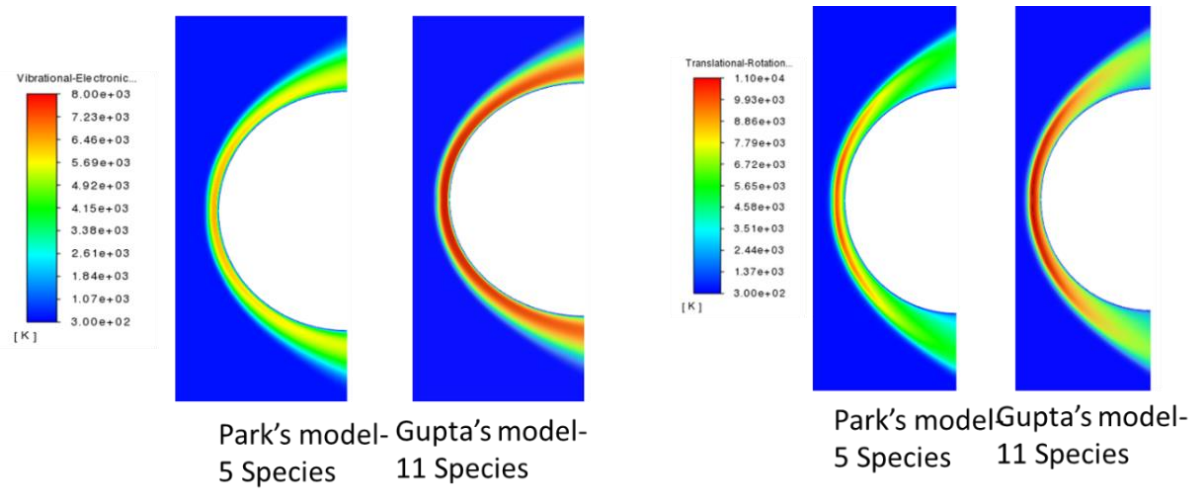

Figure 14 Temperature comparison of two different species model

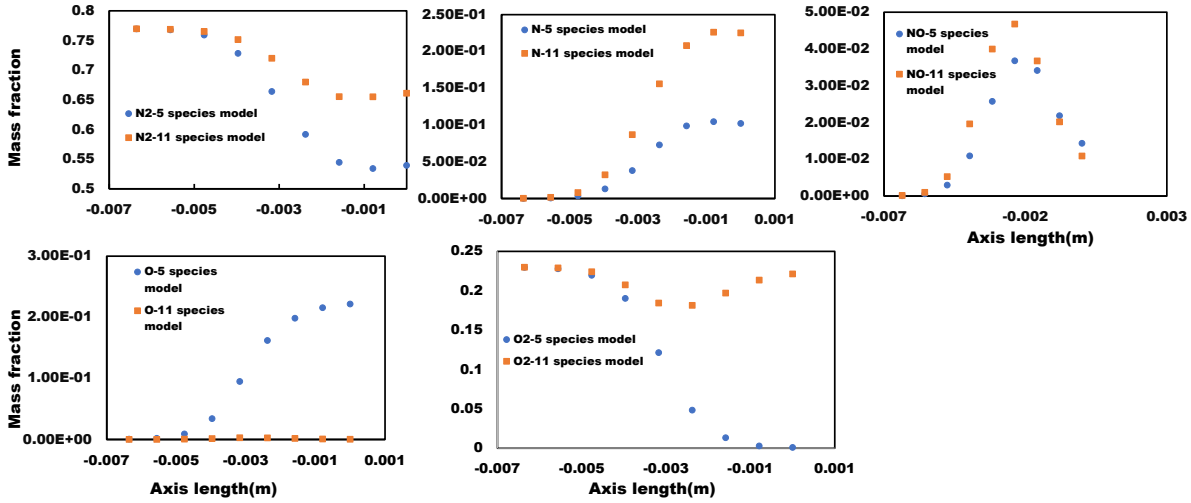

Figure 15 Mass fraction values of five different species

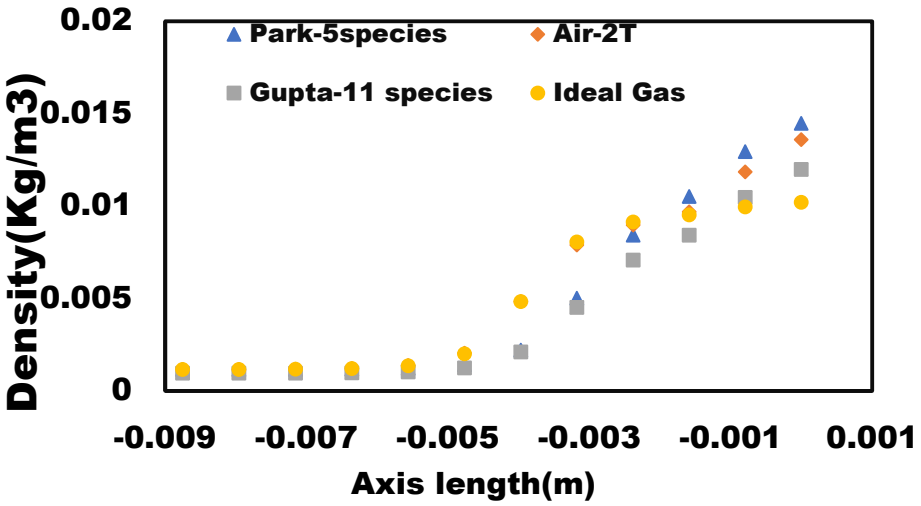

Figure 16 Density variation along the axis

Figure 16 shows density variation along the axis of the flow field. The density values are plotted using the results of four different models. The density values do not show any difference in density value as far away from the station point location and bow shock from the nose cone. The larger variation in density values can be observed in the case of an ideal gas and two-temperature air (AIR2T) used as the free stream fluid. But the variation of density values predicted by Park's model and Gupta's models are less expected near the stagnation point. The variation in density is nothing but a shock that stands off distance from the stagnation point. The variation in shock standoff with the model can be seen in the Figure 16. The increase in density values of the species model after the bow shock leads to smaller shock standoff distance as compared to non-species model.

Changing the chemical reaction species model significantly influences heat flux and shock standoff distance in hypersonic flow. Comparative simulations using Gupta's 11-species model and Park's 5-species 93 model reveal noteworthy differences. Gupta's model, with its increased

species complexity, predicts higher heat flux, temperatures, and reduced shock standoff distance, particularly near the stagnation point. In essence, it emphasizes the critical role that chemical reactions play in influencing the behavior of hypersonic flow and underlines the importance of choosing an appropriate chemical reaction species model for such simulations.

4.3 Unveiling the Cooling Impact: Does Sco2 Cool the Leading Edge?

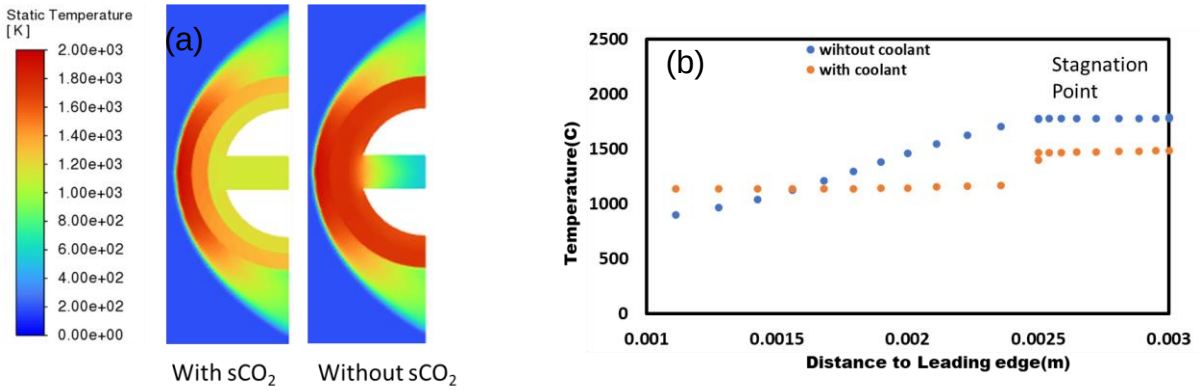

Figure 17 (a) Temperature contour (b)static temperature along the axis

The investigation into the effectiveness of sCO2 in cooling the leading edge is conducted through comprehensive numerical simulations, where the sCO2 space is treated as a solid medium to replicate real-world conditions accurately. The simulations involve two distinct cases, each exposed to an external flow at Mach 7. The visual insights gained from temperature contour plots distinctly showcase that, in the absence of sCO2 coolant, the leading-edge experiences significantly higher temperatures. This observation underscores the critical role played by sCO2 in actively mitigating extreme heat at the leading edge, making it an essential component for effective thermal management in hypersonic vehicles.

To delve deeper into the quantitative aspects of the simulations, static temperature profiles along the axis are meticulously examined. The comparison between the two cases highlights a consistent trend where the scenario with sCO2 coolant consistently maintains lower

temperatures along the leading edge. This temperature reduction is crucial for preventing structural damage and ensuring optimal aerodynamic performance. Notably, the coolant case exhibits a substantial reduction in the maximum temperature by 300K compared to the scenario without sCO2, emphasizing the significant cooling effect provided by sCO2.

These detailed findings contribute valuable insights into the efficacy of sCO2 as a cooling agent for hypersonic leading edges. The active role of sCO2 in reducing temperatures along the leading edge is pivotal for enhancing the overall efficiency and safety of hypersonic vehicles, providing a compelling case for the continued exploration and implementation of sCO2 in aerospace applications.

4.4 Effects of Free Stream Mach Number

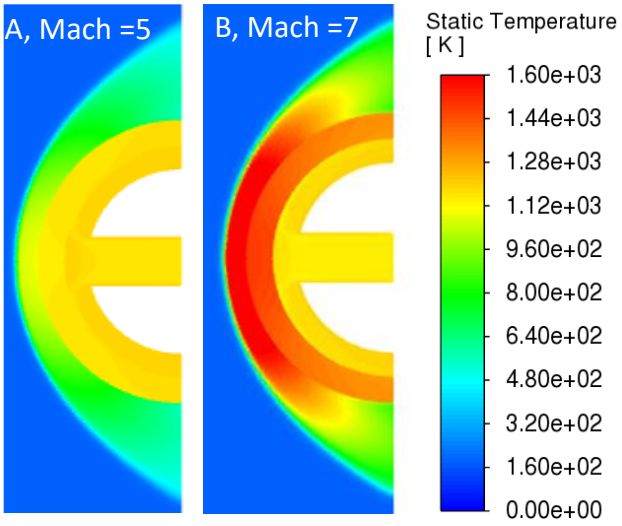

Figure 18 Temperature Contour around the Leading Edge

In this section, the results of an increase in free-stream Mach number for 5 to 7 are shown and discussed. An increase in Mach number increases the temperature of the leading edge as shown in Figure 18 and Figure 19. However, the properties of sCO2 are sensitive near-critical regions with temperature variations [16, 29]. An increase in free-stream Mach number increases the

temperature gradient across the wall. The Surface heat transfer coefficient is plotted for the two cases with different Mach numbers as shown in Figure 16. It is observed that the heat transfer coefficient is decreasing rapidly near the high-temperature region and increases in the aft region. The variation in heat transfer coefficient, with a rapid decline near the high-temperature leading edge followed by an increase in the aft section, is explained by the interplay of complex fluid dynamics and thermodynamics, primarily influenced by the behavior of the boundary layer. At the boundary layer's inception, air near the solid surface gradually transitions from zero velocity to free-stream velocity. The heightened temperature in the high-temperature region near the leading edge, particularly at high Mach numbers, results from compression and friction, causing a thinner boundary layer due to air expansion. This thin boundary layer limits heat transfer, leading to a reduced heat transfer coefficient. In the aft region, as the boundary layer thickens and the air cools due to expansion and mixing, the heat transfer coefficient begins to rise. This observed pattern is driven by variations in boundary layer thickness, temperature distribution, and fluid properties. It is fundamental in high-speed, high-temperature environments and holds significance for designing efficient thermal protection systems and optimizing aerodynamic performance.

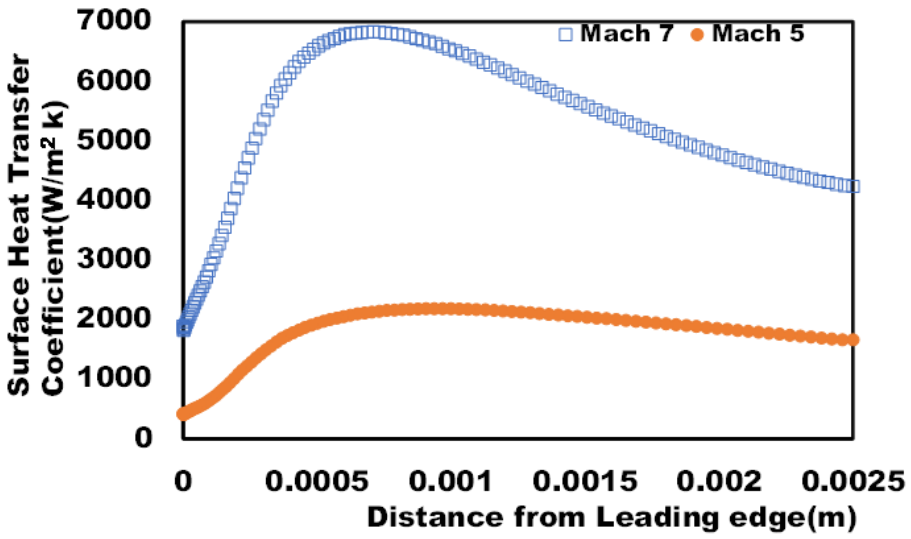

Figure 19 Surface Heat Transfer Coefficient around the Leading Edge

The heat transfer coefficient increases with Mach number because higher Mach numbers involve faster airflows with more kinetic energy and elevated temperatures due to compression. This results in a greater temperature difference between the solid surface and the fluid, leading to a higher heat transfer coefficient.

The heat transfer coefficient increases with Mach number primarily due to the increased kinetic energy and temperature of the airflow at higher Mach numbers. Here's a more detailed explanation:

1. Velocity and Kinetic Energy: As the Mach number increases, the velocity of the fluid (air) relative to the speed of sound also increases. This implies that the fluid particles are moving at higher speeds. The kinetic energy of these faster-moving particles is directly proportional to the square of the velocity. So, at higher Mach numbers, the kinetic energy of the fluid is significantly greater.

2. Thermodynamic Effects: In addition to higher velocities, higher Mach numbers correspond to increased temperatures. This is a consequence of compression, which occurs as the fluid accelerates to supersonic or hypersonic speeds. As the fluid is compressed, its temperature rises due to the conversion of kinetic energy into thermal energy. This elevated temperature of the fluid contributes to increased heat transfer.
3. Heat Transfer Relationship: The heat transfer coefficient (h) is a measure of how effectively heat is transferred from a solid surface to a fluid (in this case, air). The rate of heat transfer is related to the difference in temperature between the solid surface and the fluid, as well as the properties of the fluid. At higher Mach numbers, the temperature of the fluid is higher, leading to a greater temperature gradient between the solid surface and the fluid. According to the convective heat transfer equation:

$$Q = h * A * \Delta T$$

Where:

- Q is the heat transfer rate.
- h is the heat transfer coefficient.
- A is the surface area.
- ΔT is the temperature difference.

The increased temperature difference (ΔT) at higher Mach numbers leads to a higher heat transfer rate (Q), and consequently, a higher heat transfer coefficient (h).

In summary, the heat transfer coefficient increases with Mach number because higher Mach numbers result in both increased fluid velocity (kinetic energy) and elevated fluid temperature.

These factors contribute to a greater temperature gradient between the solid surface and the fluid, leading to more efficient heat transfer and a higher heat transfer coefficient.

4.5 Sco2 Coolant: Heat Transfer and Cooling Performance Over Air

Initial investigations have been undertaken to numerically evaluate the effectiveness of air and supercritical carbon dioxide (sCO2) as coolants. The tests were conducted at Mach number 7 under free stream conditions at an altitude of 40 km. Figure 13 illustrates the temperature distribution along the leading-edge axis, providing insights into cooling performance. The findings reveal that transitioning from air to sCO2 results in similar behavior, with certain regions experiencing reduced temperatures.

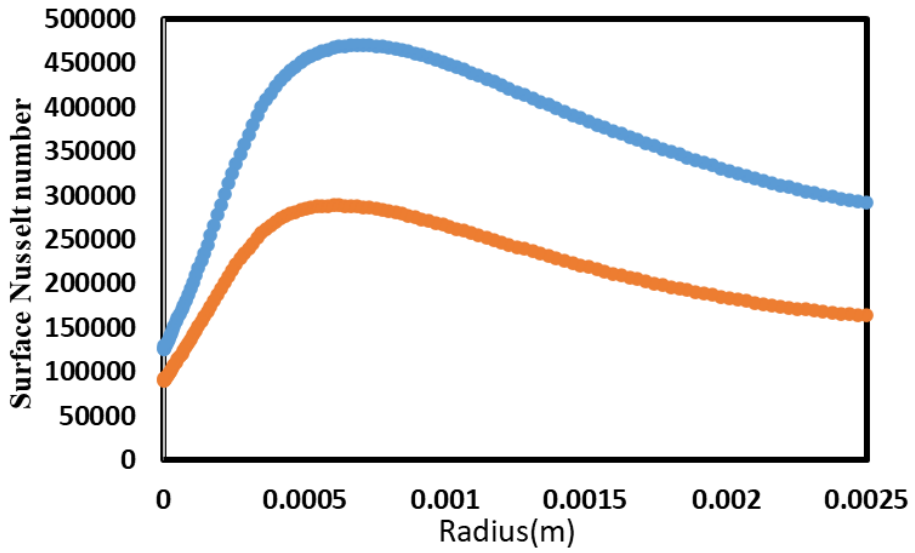

Figure 20 sCO2 Vs air

Figure 20 visually represents the impinging flow on a concave leading edge, offering an optimistic observation for employing sCO2 as a coolant in the current research. Notably, these trends are specific to the cases studied here. Further investigations will meticulously explore other parameters such as pressure and temperature. It's important to highlight that sCO2

demonstrates a higher heat transfer coefficient owing to its superior thermal conductivity and heat capacity in comparison to air. This characteristic significantly influences the effectiveness of heat transfer in the system.

4.6 The Influence of Thermal Barrier Coatings

In hypersonic flight, the metal employed may require thermal barrier coatings to shield it from the extreme heat and oxidation. To assess the effects of these Thermal Barrier Coatings (TBCs), a numerical simulation was conducted for a Mach 7 hypersonic flow scenario. In this simulation, pure tungsten alloy used as the metal, and a TBC made of reinforced carbon composite with a thickness of 500 μm is applied. This TBC is characterized by high insulating properties, boasting a low thermal conductivity.

The temperature distribution along the stagnation streamline illustrates the influence of the TBC, comparing the results obtained with and without the TBC. Notably, the maximum temperature experienced by the tungsten metal is reduced when the TBC is applied compared to when it is absent. However, it's important to highlight that the maximum temperature at the leading-edge increases with the presence of the TBC, potentially raising concerns about delamination.

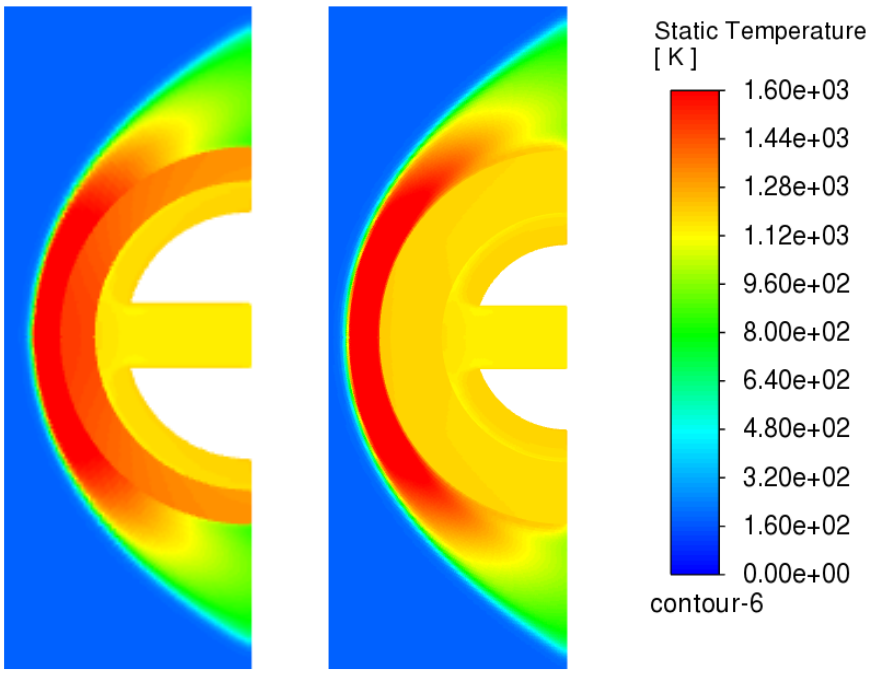

Figure 21 Temperature Contour around the Leading Edge for Mach 7 using sCo_2 as Coolant.

To prevent the leading metal from melting, ablating materials are used as the thermal barrier coating. Generally, Reinforced Carbon/Carbon (RCC) ceramic is used as the thermal barrier coating for hypersonic vehicles. In the current case, Reinforced Carbon-Carbon (RCC) is used as the TBC as the external material. The temperature distribution is shown in Figure 21 and Figure 22. The general observation of the investigation is as follows: The presence of the coating decreases the metal temperature and increases the overall temperature of the leading edge. The temperature decreases from the hot external environment to the metal interface. This gradual decrease in temperature minimizes the thermal shock and stress on the metal, which can occur when it is exposed directly to extreme temperatures. Also, TBCs possess low thermal conductivity, impeding heat transfer from the hot external environment to the underlying metal during hypersonic flight. The presence of the TBC creates a thermal gradient through its thickness. The temperature decreases from the hot external environment to the metal interface.

This gradual decrease in temperature minimizes the thermal shock and stress on the metal, which can occur when it is exposed directly to extreme temperatures.

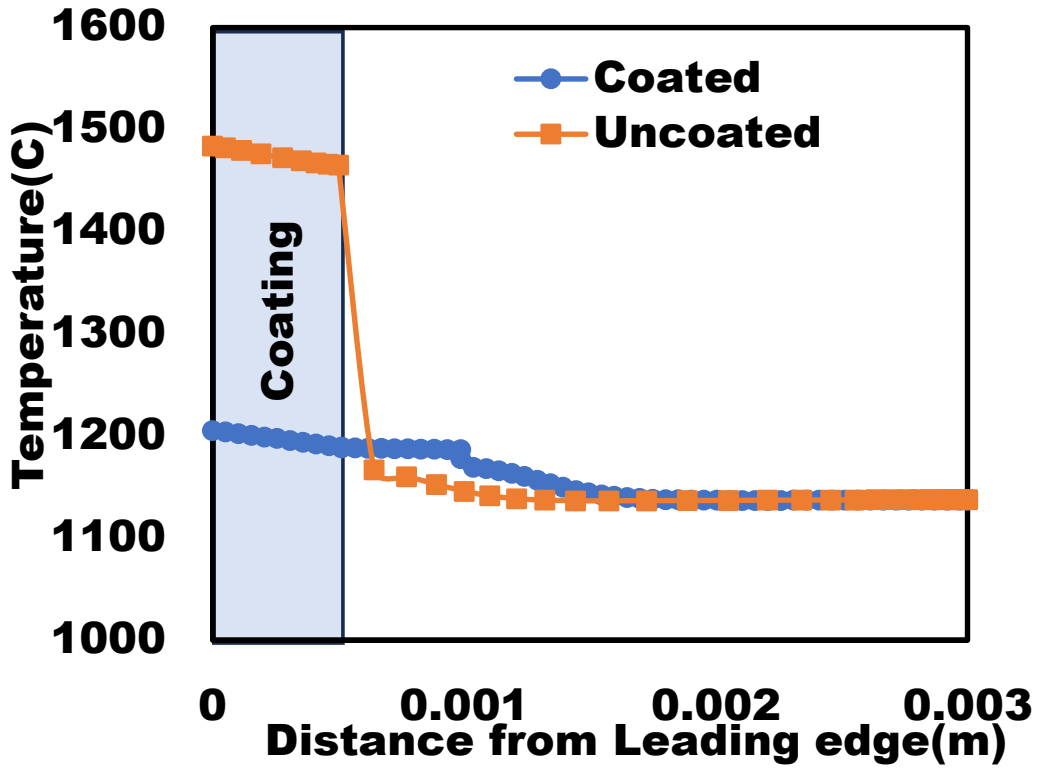

Figure 22 Temperature Distributions along the Axis Line of a Leading-edge for TBC-coated and Uncoated

4.7 Effects Of Sco2 Jet Impingement Tube to Nose Cone Length(Z/D) On Nu

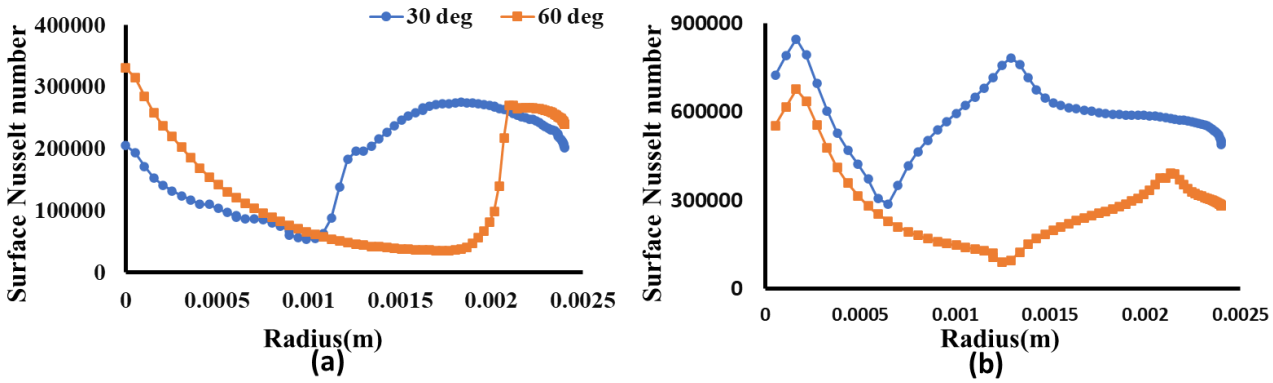

Figure 23 Nusselt number along the Leading-edge surface of the nose cone (a) Z/D = 1 (b) Z/D = 5

The Figure 23 shows the influence of jet impingement angle on a hypersonic vehicle nose cone for a Reynolds number value of 22500. The impingement jet inlet is sent with a mass flow rate of 44 Kg/g/h. and kept at the pressure and temperature well above critical conditions at 199 atm and 1200K. The figure and b show Nusselt's values for Z/D values of 1 and 5. The peak Nusselt's number at the stagnation point of the nose cone increase with the increase in Z/D values from 1 to 5. It is observed that Nusselt's values in the case of Z/D = 5 is higher than the values in the case of Z/D=1. The peak Nusselt's number in the case of z/D is equal to 5 almost double the value compared to Z/D values of 1. It is inferred that for the given operating conditions Z/D =5 is better in the heat transfer perspective as compared to smaller Z/D values. Extensive parametric will be conducted to find the optimal Z/D values for the current operating conditions. It is concluded that the heat transfer is highly dependent on the values of relative tube to the nose cone's surface (Z/D).

But the peak Nusselt's number is giving inconclusive results when compared between the two impingement angles 30 deg and 60 deg. The peak Nusselt's number values change according to the Z/D values. In the case of Z/d =5 the peak Nusselt's of 60 deg case is higher than the 30 deg case. But in the case Z/D=1 the peak Nusselt's number of 30 deg case is less than the 60 deg impingement case.

Z/D = 5 offers superior heat transfer performance compared to smaller Z/D values due to its effect on the boundary layer characteristics and the way it influences the flow dynamics. Here's why:

1. **Boundary Layer Thickness:** The Z/D ratio, where Z is the distance between the impinging jet outlet and the surface and D is the diameter of the impinging jet, has a direct impact on the thickness of the boundary layer. A larger Z/D ratio means that the

impinging jet is positioned farther from the surface. This greater distance allows the boundary layer to develop and thicken more effectively. In contrast, smaller Z/D ratios result in the impinging jet being closer to the surface, causing a thinner boundary layer.

2. **Turbulent Mixing:** A thicker boundary layer offers more space for the turbulent mixing of the impinging jet with the boundary layer flow. This enhanced mixing leads to increased heat transfer rates. With Z/D = 5, there is more room for turbulent eddies and vortices to develop within the boundary layer, promoting efficient heat transfer.

3. **Enhanced Convection:** The greater distance in Z/D = 5 creates a longer contact time between the high-velocity impinging jet and the boundary layer. This prolonged contact time allows for improved convective heat transfer, as the fluid has more opportunities to exchange energy with the solid surface. Consequently, more heat is transferred from the solid surface to the fluid, leading to higher Nusselt numbers and superior heat transfer performance.

4. **Reduced Heat Transfer Inhibition:** Smaller Z/D values, where the jet is closer to the surface, can inhibit heat transfer due to limited space for turbulent mixing. This proximity can restrict the ability of the impinging jet to efficiently penetrate and disrupt the boundary layer, resulting in reduced heat transfer effectiveness.

In summary, Z/D = 5 is favored for superior heat transfer performance because it allows the boundary layer to develop fully, encourages turbulent mixing, extends the contact time between the impinging jet and the surface, and minimizes the inhibiting effects that closer impingement can have on heat transfer. This understanding is essential for optimizing cooling and heat

transfer systems in various engineering applications, especially in the design of hypersonic vehicles.

4.8 Effects Of Sco2 Jet Impingement Angle on Nu

Velocity flow field is used to explain the trends observed in the Nusselt's number in the Figure 24. It is observed that the Nusselt's number is directly proportional to the velocity of the flow field inside of the coolant region. The Nusselt's number is higher at the impingement point of the jet. Nusselt's values are decreasing as it goes further away from the impingement point. The 'v' shaped recovery of Nusselt's values is observed at the second impingement point of the flow field. The 'v' shaped recovery of Nusselt's number happens earlier in the case of 30 deg case as compared to the 60 deg.

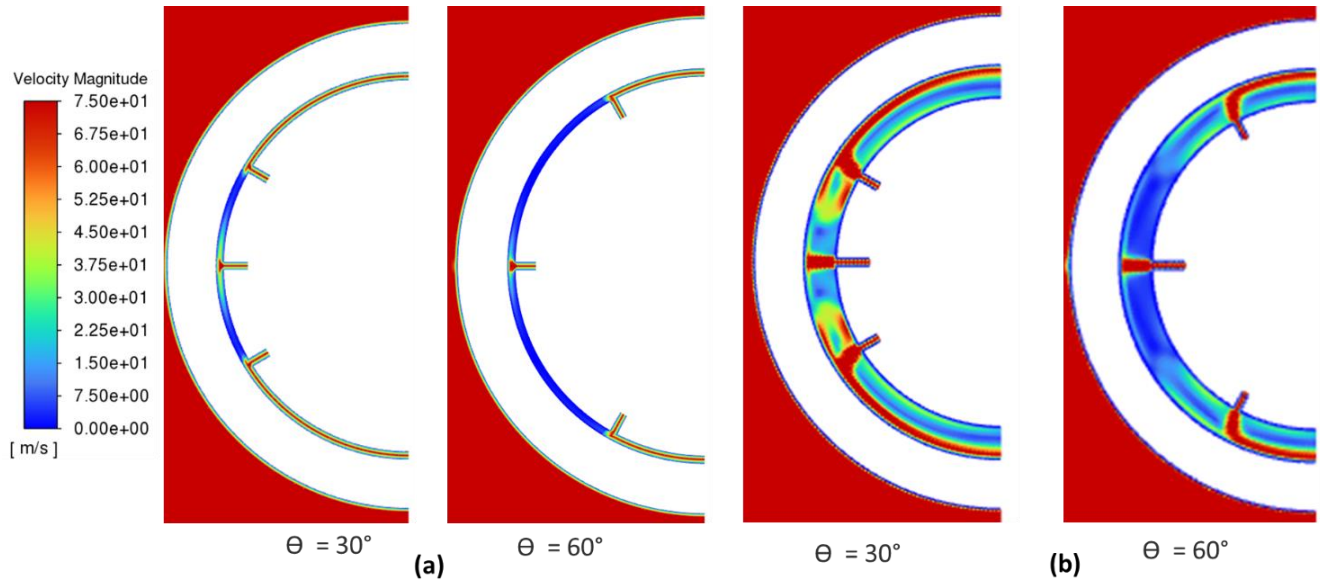

Figure 24 Velocity flow field along the Leading-edge surface of the nose cone (a) Z/D = 1 (b) Z/D = 5

It can be explained with the help of velocity field visualization. The second impingement point is further away from the stagnation point in the case of 60 deg as compared to the 30 deg. The observed behavior is common to all the impingement angle cases tested. It can be inferred that

the distance between two impingement points should be kept as close as possible to achieve better heat transfer. Another observation with the use of area averaged Nusselt's number of all the cases. It is observed that area averaged Nusselt's number along the nose cone's surface is higher in the 30 deg impingement case than others. This observation is common for both the Z/D values from 1 and 5.

To test the above-mentioned theory of keeping the distance between the impingement as close as possible to increase the Nusselt's and heat transfer. A new type of simulation is done by combing the impingement angle of 30 deg and 60 deg as shown in Figure 25 below. As a result, the area Nusselt's number is higher in the current stimulation by combining the 30 deg and 60 deg impingement angle in a single model.

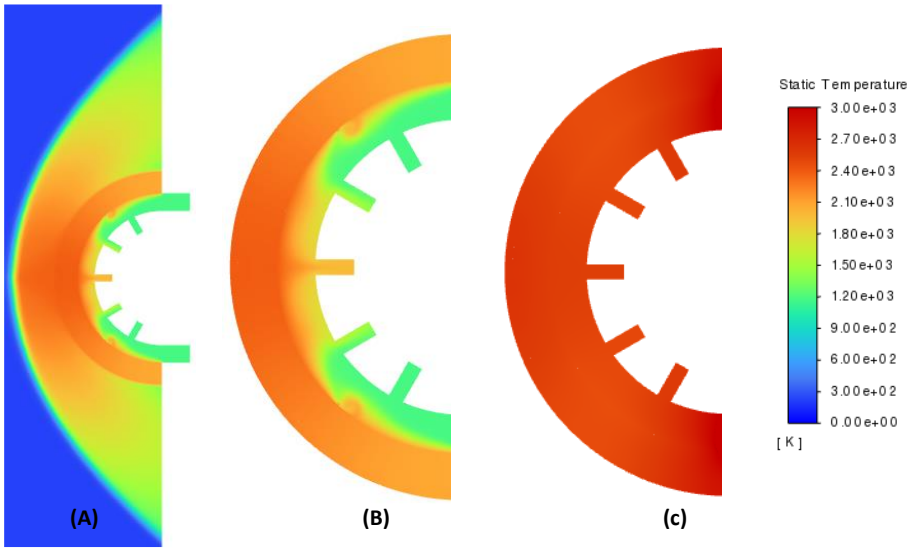

Figure 25 Temperature Contours (A) Complete Solid and fluid regions (B) metal region with impingement jet, (C) a metal region without impingement jet

This section shows the effect of impingement jets on cooling solid metal. Figure 25 shows static temperature contours with sCO2 impingement and without impingement. It is obvious that the solid metal with the cooling experiences reduced temperature on the solid surface as

compared to the solid metal without cooling. In further studies, the injection rates of the jets will be changed to study their effects on the heat transfer performance.

The "V" shaped Nusselt recovery observed at the second impingement point, with the 30-degree angle exhibiting the "V" shape earlier compared to the 60-degree angle, can be explained by the interplay of fluid dynamics and the positioning of the impingement points. Here's the scientific reasoning for this phenomenon:

Impingement and Mixing: When a high-velocity jet impinges on a solid surface, it creates a zone of intense mixing and disruption in the boundary layer. This leads to higher heat transfer rates at the impingement point, resulting in elevated Nusselt numbers. The intense mixing causes a local peak in heat transfer near the impingement point.

Flow Reattachment: As the flow continues downstream from the impingement point, it starts to reattach to the solid surface. This reattachment process occurs due to pressure and velocity variations. In the context of heat transfer, this reattachment marks a shift from the region of strong impingement to a region where the flow separates less, reducing the heat transfer rate.

Nusselt Recovery: The "V" shaped Nusselt recovery is a consequence of this flow reattachment. After the initial peak at the impingement point, the Nusselt number decreases as the flow detaches and moves away. However, as the flow begins to reattach further downstream, it creates a secondary region of increased heat transfer, resembling the shape of a "V."

Effect of Impingement Angle: The positioning of the impingement points, influenced by the impingement angle, plays a significant role. A 30-degree angle results in the second

impingement point occurring closer to the stagnation point. This proximity to the stagnation point means that the "V" shaped Nusselt recovery happens earlier, as the flow reattaches sooner.

Closer Impingement Points: The consistent observation of this behavior across impingement angle cases suggests that keeping the impingement points as close as possible to the stagnation point is advantageous for heat transfer. Closer impingement points allow for more rapid reattachment of the flow and the creation of the secondary region of enhanced heat transfer, resulting in a higher Nusselt number.

Area-Averaged Nusselt Numbers: The area-averaged Nusselt numbers are higher for the 30-degree impingement case because the early "V" shaped Nusselt recovery results in a more significant overall increase in heat transfer.

Combining Impingement Angles: Combining 30-degree and 60-degree impingement angles in a single model leverages the advantages of both angles, resulting in a more comprehensive heat transfer effect. This combination increases area averaged Nusselt numbers as it maximizes the benefits of heat transfer enhancements at both impingement points.

In summary, the "V" shaped Nusselt recovery phenomenon arises from the interaction of impingement, flow reattachment, and the positioning of impingement points. Closer impingement points near the stagnation point enhance heat transfer, resulting in higher Nusselt numbers. Combining multiple impingement angles in a single model can further optimize heat transfer performance.

CHAPTER 5

HEAT TO POWER CONVERSION: $sC0_2$ CYCLE

Hypersonic vehicles are aircraft that fly faster than five times the speed of sound (Mach 5). They have various potential applications, such as space exploration, military operations, and rapid transportation. However, they also face many technical challenges, such as aerodynamic heating, propulsion, and cooling. One of the possible solutions for cooling the hypersonic vehicle is an active cooling system that utilizes the sCO2 Brayton cycle. The sCO2 Brayton cycle can provide both power generation and heat rejection for the vehicle while reducing the weight and complexity of the system.

The design and operation of hypersonic vehicles pose unique challenges, especially in the efficient conversion of heat generated during high-speed flight into usable power. In this chapter, the specifics of the $SC0_2$ cycle, a cutting-edge thermodynamic cycle tailored for hypersonic applications. The $SC0_2$ cycle addresses the need for effective heat to power conversion, ensuring optimal performance and energy utilization in the demanding environment of hypersonic flight. The supercritical carbon dioxide (sCO_2) power cycle is a highly efficient, advanced thermal cycle that uses sCO_2 as the working fluid. The term "supercritical" describes the state of carbon dioxide above its critical temperature of 31.1°C and critical pressure of 73.8 atmospheres, making it neither a liquid nor a gas. After the sCO2 passes through a turbine, it is cooled and then re-pressurized before returning for another pass. The turbine drives a generator for power production.

The basic idea of using the sCO2 Brayton cycle for hypersonic vehicles is to extract heat from the vehicle's skin and use it to drive a turbine-alternator-compressor (TAC) unit that produces

electricity. The electricity can then be used to power the vehicle's subsystems, such as avionics, sensors, and communications. The sCO2 working fluid is then cooled by a heat exchanger and recycled back to the compressor. The heat exchanger can be either air-cooled or water-cooled, depending on the availability of the cooling medium. The sCO2 Brayton cycle can also be integrated with other propulsion systems, such as scramjets or ramjets, to improve their performance and efficiency.

5.1 Advantages of sCO_2 Cycles

There are several advantages of using the sCO2 Brayton cycle for hypersonic vehicles, such as:

- Higher efficiency: The sCO2 Brayton cycle can achieve higher thermal efficiency than conventional steam or gas turbine cycles, because of its higher operating temperature and lower compression work. The theoretical efficiency of the sCO2 Brayton cycle can reach up to 50%, compared to 30% for steam or gas turbine cycles.

- Lower emissions: The sCO2 Brayton cycle does not produce any harmful emissions, such as carbon dioxide, nitrogen oxides, or particulates, because it uses a closed-loop system with no combustion. The sCO2 working fluid is also nontoxic and stable and does not contribute to the greenhouse effect.

- Smaller size: The sCO2 Brayton cycle can reduce the size and weight of the power generation and cooling system, because of its higher density and lower specific volume than steam or air. The sCO2 working fluid can also operate at higher pressures, which reduces the size of the TAC unit and the heat exchanger. The smaller size of the system can improve the aerodynamics and maneuverability of the hypersonic vehicle.

- Lower cost: The sCO2 Brayton cycle can lower the cost of the power generation and cooling system, because of its simpler design and fewer components. The sCO2 working fluid is also cheaper and more abundant than other working fluids, such as helium or water. The lower cost of the system can make the hypersonic vehicle more affordable and accessible.

5.2 Main Components of Sco2 Cycles

The supercritical carbon dioxide Brayton cycle (sCO2 CBC) system has four main components as show in Figure 26a

Compressor: The compressor increases the pressure of the low-pressure, low-temperature sCO2 to a high-pressure, low-temperature state.

Heat exchanger: The high-pressure, low-temperature sCO2 is passed through a heat exchanger where it absorbs heat and becomes a high-pressure, high-temperature sCO2.

Turbine: The high-pressure, high temperature sCO2 expands in a turbine, producing work that can be converted to electricity.

Cooler: The low-pressure, high temperature sCO2 is cooled at constant pressure in the cooler before it is sent back to the compressor.

5.3 The Supercritical Carbon Dioxide Brayton Cycle

The supercritical carbon dioxide Brayton cycle (sCO2 CBC) is an innovative approach to converting thermal energy into electrical energy, employing supercritical carbon dioxide (sCO2) as the working fluid. Leveraging the distinctive properties of sCO2, this cycle proves exceptionally well-suited for efficient energy conversion. Notably, the sCO2 CBC represents

a highly efficient thermodynamic process, capturing considerable attention in recent years due to its distinct advantages over traditional steam or gas turbine cycles.[63–65]

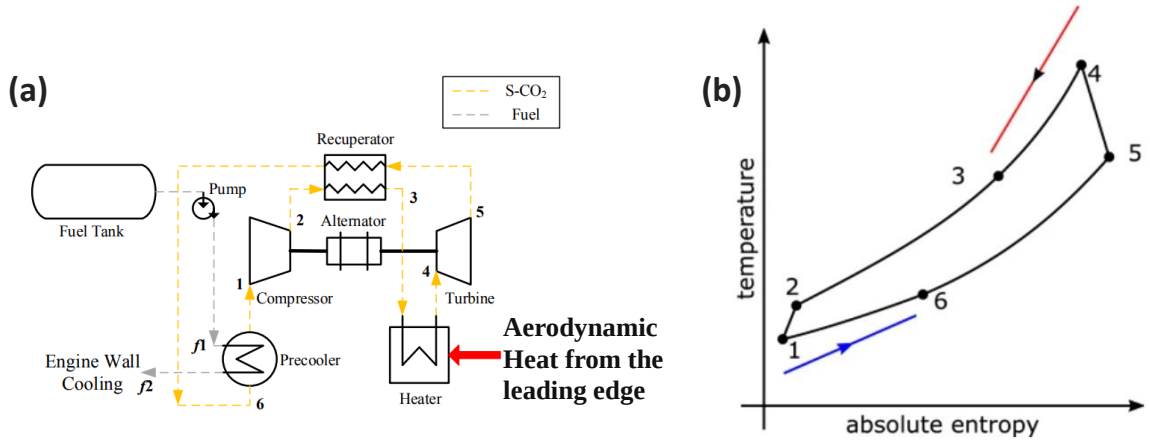

Figure 26 (a)Simple regenerated sCO_2 Closed Brayton cycle system[66] **(b) T-s diagram.**[67]

1-2 Compression

The cycle as shown in Figure 26 begins with the compression of the low-pressure, low temperature sCO2 (state 1) in a compressor. The sCO2 is compressed to a higher pressure (state 2), which increases its temperature due to the work done on the fluid. This process is adiabatic, meaning no heat is exchanged with the surroundings. The efficiency of this stage is largely dependent on the compressor design and operation.

Compression (1-2): The compression process is governed by the isentropic relation for an ideal gas:

$$T_2 = T_1 \times \left(\frac{P_2}{P_1}\right)^{\left(\frac{\gamma-1}{\gamma}\right)}$$

1. The isentropic efficiency of the compressor:

$$\eta_C = \frac{h_2 - h_1}{h_{2s} - h_1}$$

where h_1, and h_2, are the enhalpies before and after the compression (T_1) and T_2 are the temperatures before and after compression, (P_1)and $P_2$are the pressures before and after compression, and γ is the ratio of specific heats.

$$\rho_C = \frac{p_1}{p_2}$$

2-3 Recuperator (Hot Side)

The high-pressure, high temperature sCO2 from the compressor outlet (state 2) then enters the hot side of a recuperator. The recuperator is a type of heat exchanger that transfers heat from the hot sCO2 to the cooler sCO2 returning from the turbine (state 5). This process increases the temperature of the sCO2 (state 3) before it enters the heater, improving the overall efficiency of the cycle by reducing the amount of external heat required.

Recuperator (Hot Side) (2-3): The heat transfer in the hot side of the recuperator can be calculated using the equation:

$$Q = \dot{m} \times C_p \times (T_2 - T_3)$$

where $\dot{m}$ is the mass flow rate, C_p is the specific heat at constant pressure, and T_2 and T_3 are the temperatures before and after the recuperator.

$The\ recuperator\ effectiveness$:

$$\epsilon_{REC} = \frac{h_5 - h(T_2, p_6)}{h_5 - h_6}$$

3-4 Heater

The high-pressure, high temperature sCO2 from the recuperator (state 3) is then further heated in a heater. This process increases the thermal energy of the sCO2 (state 4), preparing it for expansion in the turbine. The heat source for this process can vary, ranging from conventional fossil fuels to renewable sources like solar or nuclear energy. In this study, the aerodynamics heating form slowing down hypersonic flow at the leading acts as a heat source.

$$Q_{HT} = \dot{m} \times C_p \times (T_4 - T_3)$$

4-5 Turbine

The high-pressure, high temperature sCO2 from the heater (state 4) is then expanded in a turbine. The expansion of the sCO2 results in a drop in its pressure and temperature, and the conversion of its thermal energy into mechanical work. The mechanical work can be used to drive an electrical generator or other machinery. The efficiency of this stage is largely dependent on the turbine design and operation.

The pressure ratio of the turbine:

$$\rho_T = \frac{p_5}{p_4} = \rho_C \prod_{i=1}^{n} (1 - x_i)$$

T*he isentropic efficiency of the turbine*:

$$\eta_T = \frac{h_4 - h_{5s}}{h_4 - h_5}$$

5-6 Recuperator (Cold Side)

The low-pressure, low temperature sCO2 from the turbine outlet (state 5) then enters the cold side of the recuperator. Here, it absorbs heat from the hot sCO2 coming from the compressor

(state 2), increasing its temperature (state 6) before it enters the pre-cooler. This process improves the overall efficiency of the cycle by reducing the cooling load on the pre-cooler.

6-1 Pre-cooler

Finally, the sCO2 from the recuperator (state 6) is cooled down in a pre-cooler before it returns to the compressor (state 1), completing the cycle. The pre-cooler removes the remaining heat from the sCO2, bringing it back to its initial low-pressure, low-temperature state. This process ensures the sCO2 is at the optimal temperature for compression, improving the overall efficiency of the cycle.

the sCO2 Brayton cycle is a promising technology for power generation due to its high efficiency and flexibility. Its unique use of sCO2 as the working fluid, coupled with the recuperative heat exchange process, allows for significant improvements in thermal efficiency compared to traditional power cycles. As research and development continue, the sCO2 Brayton cycle holds great potential for a more sustainable and efficient energy future.

The thermal efficiency of the simple recuperated layout:

$$\eta_{th;SRL} = \frac{Q_{HT}}{m_{CO2}(w_T - w_C)} = \frac{h_4 - h_3}{(h_4 - h_5) - (h_2 - h_1)}$$

The mass flow rate ratio of carbon dioxide to fuel for the simple recuperated layout:

$$g_{SRL} = \frac{m_f}{m_{CO2}} = \frac{h_6 - h_1}{h_{f2} - h_{f1}}$$

The electric power of the simple recuperated layout with finite cold source:

$$P_{SRL} = \frac{m_{CO2}(w_T - w_C)}{\eta_G} = \frac{m_f(h_6 - h_1)}{h_{f2} - h_{f1}}$$

5.4 sCo_2 Properties and A Potential Thermodynamic Power Cycle

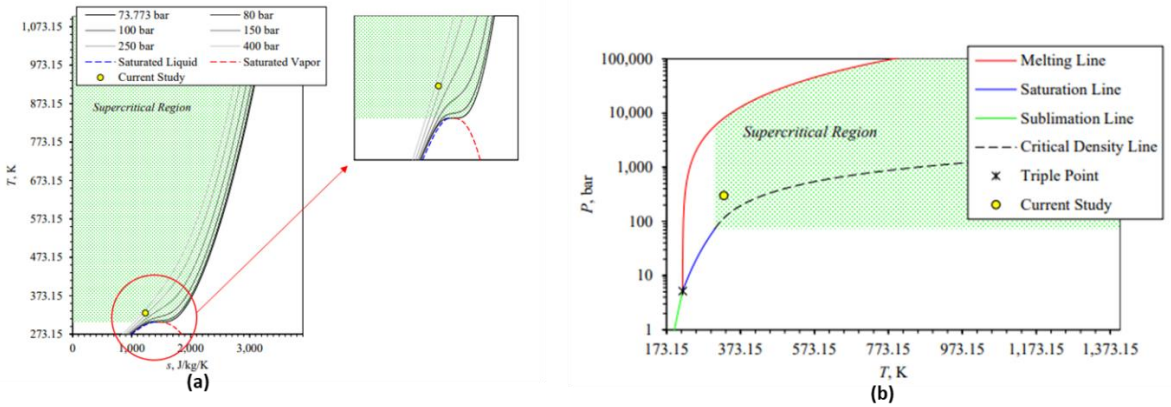

Figure 27 (a) CO_2 T-S diagram (b) CO_2 P-T diagram

In any supercritical fluid, the distinction between the liquid phase and gas phase disappears gradually. The phase change process of CO2 from subcritical to supercritical is shown in Figure 4. Also, The Thermo-physical properties of sCO2 dramatically change with the change in pressure and temperature. The real gas properties should be used while the heat transfer properties and usage of sCO2 in power cycles are explained in detail in the review paper by Cabeza et al. [17]. It is also shown that heat transfer enhancement can be achieved for various geometries using sCO2.

Even though this paper is primarily focused on the heat removal for leading-edge cooling, the thermal parameters used for the simulation are based on a potential sCO2 simple Brayton cycle that could be used for converting the acquired heat into useful work. The sCO2 power cycle is one of the promising power systems for the next generation of a power conversion system with potential applications in a multitude of different fields [18, 19]; including, but not limited to waste heat recovery [20, 21]. The sCO2 power cycle is a gas-based power cycle with many advantages compared to other conversion cycles. The overall system is compact with high cycle efficiency for operation parameters above 450 °C (turbine inlet temperature). The overall cycle layout consists of a compressor (point 5 and 6), a turbine (point 2 and 3), a cooler (point

4 and 5), a primary heat exchanger (point 1 and 2), and a recuperative heat exchanger (point 3 and 4 on hot side and point 1 and 6 on cold side). The sCO2 power cycle has several different cycle layouts that can affect the cycle efficiency and the net power. The typical cycle layout is the simple Brayton cycle.

The input parameters of the simple Brayton cycle considered for preliminary simulation are shown in Table 3. The turbine inlet pressure is 19.7584 MPa. The sCO2 mass flow rate is 0.004 kg/s. The simulations were performed using in-house developed computer programs that were designed to optimize the Brayton power cycle with the CoolProp as a source of gas properties [22]. CoolProp is the open-source Thermophysical Property Library.

The primary heat exchanger inlet and outlet temperature and compressor inlet temperature are set as fixed variables and boundary limitations for the optimization. The compressor inlet pressure and pressure ratio are considered as optimized variables with lower and upper limits (8 and 9 MPa). The generator efficiency is considered as 96 %, clutch efficiency is 95 %, and the gearbox efficiency is 93 %. The pressure drops are not considered in the calculation, because the effect of the pressure drops will not be larger than 1 - 2 % [23].

Table 3 Input and boundary conditions of the sCO2 simple Brayton cycle.

Turbine inlet pressure	19.7584	MPa
T5	15.7	°C
T1	1200	°C
T2	1300	°C
Mass flow rate	0.024	kg/s
Compressor efficiency	75	%
Turbine efficiency	90	
Recuperator effectiveness	95	

The T-S diagram of the sCO2 simple Brayton cycle is shown in Figure 28. The results based on input and boundary conditions from Table 3 and the assumptions mentioned above are shown in Table 3. The compressor inlet pressure, respectively pressure ratio was optimized to 8.707 MPa and 2.269, respectively.

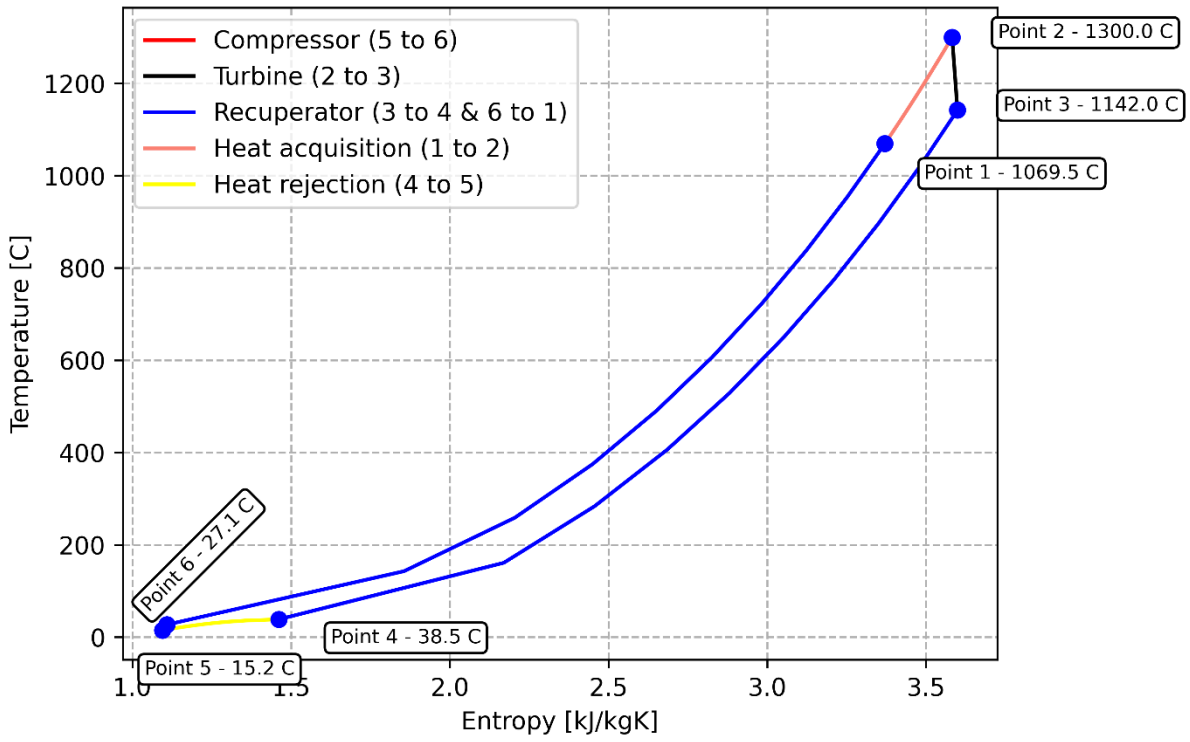

Figure 28 T-S diagram for the sCO2 simple Brayton cycle

The resulting system efficiency is 64.32 %. The net power of the system is 73.66 W for the sCO2 mass flow rate of 0.024 kg/s. Based on the results, presented in Table 4, the sCO2 cooling system has the capability to remove heat from the leading edge and transfer the energy generated by the cooling of the vehicle. While cooling is provided to the leading edge of the vehicle to allow safe operation of the hypersonic vehicle, 184.15 KJ/Kg of power are generated for use of electronics and other equipment of the vehicle.

Table 4 sCO2 simple Brayton cycle optimization results

Medium	CO2
Turbine Output	213.2825 kJ/kg
Compressor Power	16.475 kJ/kg
Heating Power	308.075 kJ/kg
Cooling Power	111.265 kJ/kg
Recuperative Heat	1453.9925 kJ/kg
Net Work	184.15 KJ/kg

This study presents a hypersonic heat-to-power sample analysis focusing on CO2 as the medium. The results reveal the potential to harness power from aerodynamic heating, with critical parameters outlined. The turbine output is recorded at 213.2825 kJ/kg, while the compressor power stands at 16.475 kJ/kg. Notably, the heating power and cooling power are measured at 308.075 kJ/kg and 111.265 kJ/kg, respectively, showcasing the dynamics of energy transfer. Recuperative heat is quantified at 1453.9925 kJ/kg, contributing to the overall understanding of the system. The network obtained is 184.15 KJ/kg. The study emphasizes the significance of coolant mass flow rate, especially in considerations related to space weight and system restrictions. It suggests the feasibility of carrying the coolant in a closed cycle to extract power. The presented sample study focuses on a 0.5 mm thickness gap, serving as a foundational exploration with small mass flow rate. This research lays the groundwork for potential extensions, including multiple series of small leading edges with pin fin arrangements as shown in Figure 29, as suggested by previous studies.[26]

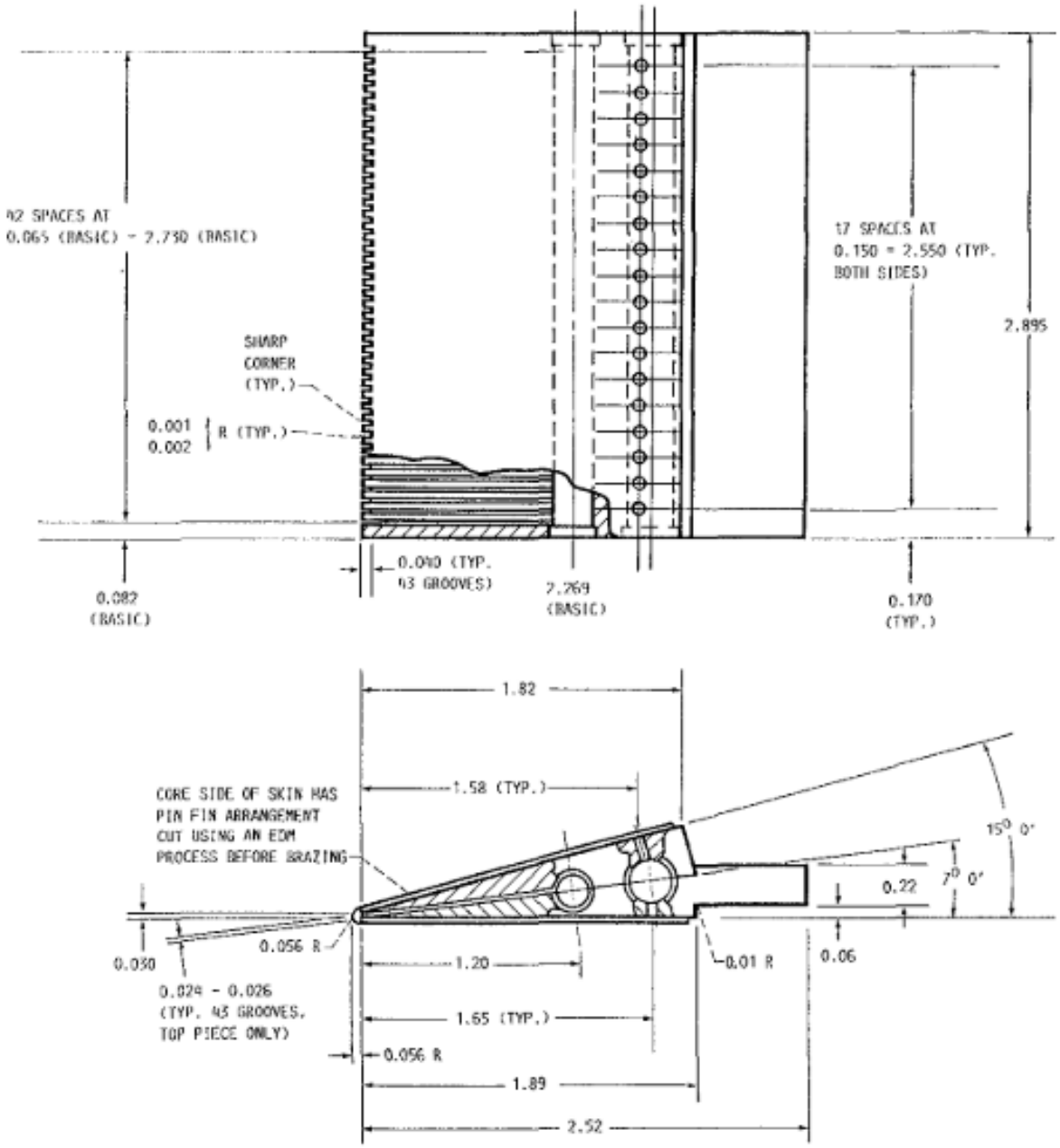

Figure 29 Impingement pin fin cooled leading edge for hypersonic vehicle (in inches)[26]

CHAPTER 6

SUMMARY AND CONCLUSION

Hypersonic thermochemical non equilibrium simulations with coupled conjugate simulation are conducted over a nose cone with sCO2 impingement. From the simulations following things are observed,

this study presents a comprehensive study of the aero and heat transfer effects of sCO2 impingement cooling in hypersonic flow scenarios. The research involves numerical simulations using a complex test setup that combines external hypersonic flow with impingement cooling.

6.1 Summary

Several key findings and conclusions can be drawn from the results and analyses presented:

1, Validation of Numerical Model: The paper begins with the validation of the numerical model, specifically for non-equilibrium flow over a nose cone. The results demonstrate good agreement between the numerical simulations and experimental data, highlighting the suitability of the chosen model for hypersonic flow simulations.

2, Influence of Chemical Reaction Species Model: The study investigates the impact of different chemical reaction species models on heat flux and flow behavior in hypersonic flow. It is observed that the 11-species Gupta's model predicts higher heat flux compared to the 5-species Park's model, indicating the significance of chemical reactions in altering flow temperatures and heat transfer.

3, Effect of Free-Stream Mach Number: The research explores how varying the free-stream Mach number affects the temperature distribution and surface heat transfer coefficient at the leading edge. It is found that increasing the Mach number results in higher temperatures and temperature gradients across the wall, with implications for heat transfer characteristics.

4, Influence of Thermal Barrier Coatings: The presence of thermal barrier coatings, such as Reinforced Carbon-Carbon (RCC), is examined. These coatings are shown to reduce the metal temperature while increasing the overall temperature of the leading edge. The study emphasizes the importance of such coatings in preventing metal melting.

5, Jet Impingement Angle and Distance (Z/D ratio): The paper investigates the impact of jet impingement angle and the distance between impingement points (Z/D ratio) on heat transfer. The results indicate that the choice of Z/D ratio significantly influences heat transfer, with larger values proving more effective in heat transfer enhancement.

6, Velocity Flow Field Analysis: Velocity flow field analysis is used to explain the observed trends in Nusselt numbers. It is shown that Nusselt numbers are directly proportional to the velocity of the flow field, with implications for optimizing impingement angles and distances.

7, Effect of Impingement Jets: The paper also examines the effect of impingement jets on cooling solid metal surfaces. The results reveal that cooling reduces the temperature on the solid surface compared to cases without cooling, highlighting the effectiveness of impingement cooling in heat transfer enhancement.

6.2 Conclusion

This dissertation presents a comprehensive exploration into the complexities of hypersonic leading-edge simulations with active cooling using sCO2. The conducted numerical simulations, corroborated by experimental data, validate the efficacy of the thermodynamic non-equilibrium two-temperature model and the selected species model in accurately capturing both external hypersonic flow and internal sCO2 coolant flow. A key finding of this research is the practicality of using sCO2 coolant to regulate metal temperatures within operational limits, a factor critical for maintaining the integrity of aerospace materials.

The study also delves into the comparative analysis between the 5-species Park model and 11-species Gupta model, establishing the former's reliability for precise flow field predictions at Mach 7. Furthermore, the research provides valuable insights into the effects of the geometric position of the sCO2 impinging jets on the leading-edge cooling. It concludes that increasing the jet distance enhances heat transfer performance, while increasing the jet angle may have the opposite effect.

Lastly, the dissertation pioneers the study of converting hypersonic vehicle heat flux to power, demonstrating the feasibility of extracting power from aerodynamic heat flux using the sCO2 cycle. This marks a significant stride towards harnessing the inherent energy of hypersonic vehicles for power generation, opening avenues for further advancements in aerospace technology. Overall, the findings presented in this dissertation contribute significantly to the evolving landscape of hypersonic vehicle design and thermal management and open new avenues for further exploration and development in the field.

CHAPTER 7

FUTURE WORK RECOMMENDATIONS

1. **Extension to Realistic Flow Scenarios:**
    - Broaden the scope of the investigation to include more intricate hypersonic flow scenarios, particularly those associated with realistic aerospace vehicle geometries. This expansion entails refining the numerical model to accommodate complex shapes and configurations, offering insights into the practical applicability of the results to aerospace applications. Employing diverse methodologies, including experimental, numerical, and analytical approaches, will contribute to a comprehensive understanding of these scenarios.
    - Enhancing the future work involves transitioning the leading-edge cooling model into a three-dimensional representation concerning heat transfer. To comprehensively investigate this cooling concept across the entire span of the leading edge, eventual modifications are necessary.
2. **Exploration of Advanced Thermal Barrier Coatings:**
    - Investigate novel thermal barrier coatings beyond Reinforced Carbon-Carbon (RCC) to assess their effectiveness in further reducing metal temperature while maintaining or improving overall leading-edge temperature. This can involve both experimental and numerical studies to validate the performance of advanced coatings under hypersonic flow conditions.
3. **Incorporation of Transient Effects:**

- Explore the transient behavior of the impingement cooling system. Investigate how the system responds during dynamic changes in flow conditions, such as during acceleration or deceleration phases. Understanding the transient effects can provide crucial information for designing adaptive cooling systems for hypersonic vehicles.

4. **Multi-Physics Analysis:**
    - Integrate multi-physics aspects into the numerical simulations by considering coupled phenomena, such as fluid-structure interaction. This can provide a more comprehensive understanding of the interplay between aerodynamics, heat transfer, and structural dynamics, particularly relevant for assessing the long-term durability of cooling systems.
5. **Optimization of Impingement Parameters:**
    - Conduct an optimization study to identify the optimal combination of jet impingement angle and the distance between impingement points (Z/D ratio). This involves exploring a range of parameter values to determine the configuration that maximizes heat transfer efficiency. The optimization process can be guided by considerations of material stress, cooling effectiveness, and overall system performance.
6. **Experimental Validation under Extreme Conditions:**
    - Perform experimental validations under extreme hypersonic conditions to verify the robustness and reliability of the numerical model. This could involve conducting impingement cooling experiments in high-temperature, high-pressure hypersonic wind tunnels, ensuring the extrapolation of findings to extreme operational scenarios.

7. **Application to Hypersonic Propulsion Systems:**
    - Extend the applicability of the research to hypersonic propulsion systems by considering the interaction between impingement cooling and propulsion-related factors. Investigate how the cooling system influences combustion efficiency, thrust, and overall propulsion system performance in the context of hypersonic flight.
8. **Development of Adaptive Cooling Strategies:**
    - Explore the development of adaptive cooling strategies that can dynamically adjust impingement parameters based on real-time monitoring of flow conditions. Adaptive strategies can enhance the resilience and efficiency of the cooling system under varying operational scenarios, contributing to the overall reliability of hypersonic vehicles.
9. **Incorporate Ablation and Surface Catalysis Analysis:**
    - Integrate ablation studies into the research to understand the effects of surface ablation on the impingement cooling system. Analyze how ablative materials respond to the hypersonic flow and impingement cooling, considering variations in material composition and thickness. Additionally, investigate the catalytic effects of the surface on heat transfer and flow behavior, exploring potential enhancements through surface catalysis.
10. **Collaboration with Industry Partners:**

- Collaborate with industry partners to implement and test the findings in practical aerospace applications. This involves working closely with aerospace manufacturers and research institutions to transition the knowledge gained from the study into real-

world engineering solutions, ensuring the relevance and impact of the research on the aerospace industry.

APPENDIX: AIAA COPY RIGHT PERMISSION

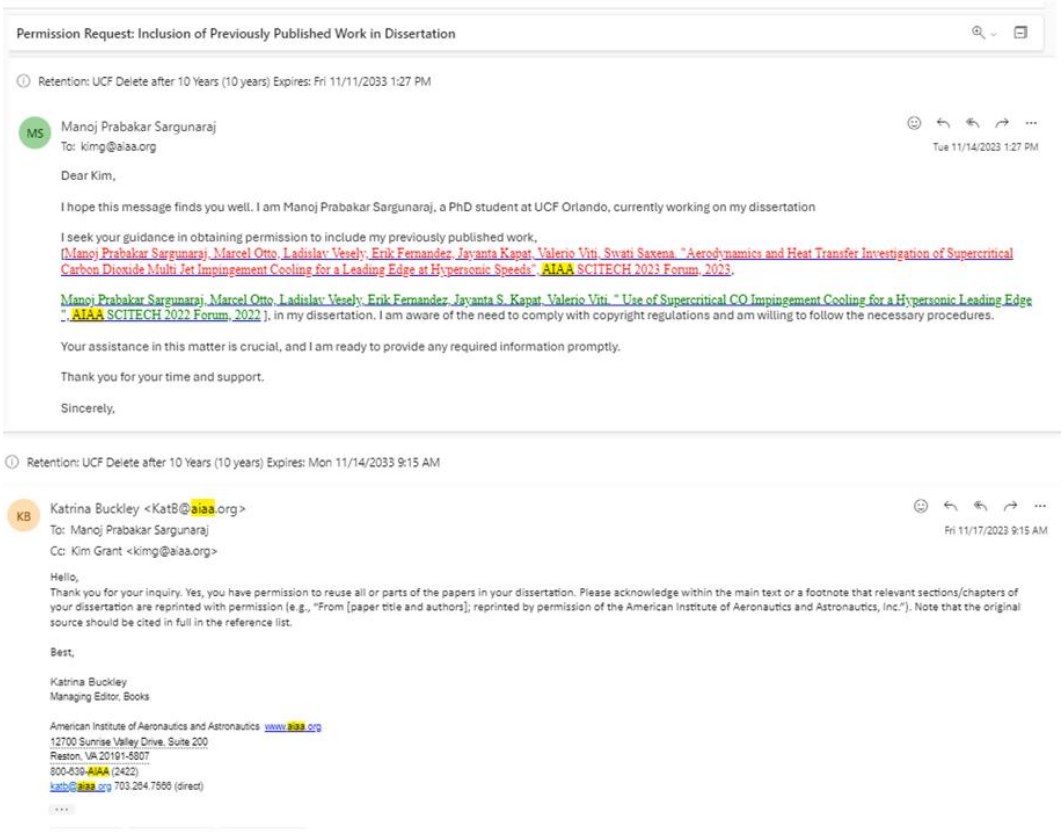

Permission Request: Inclusion of Previously Published Work in Dissertation

Retention: UCF Delete after 10 Years (10 years) Expires: Fri 11/11/2033 1:27 PM

MS Manoj Prabakar Sargunaraj
To: kimg@aiaa.org
Tue 11/14/2023 1:27 PM

Dear Kim,

I hope this message finds you well. I am Manoj Prabakar Sargunaraj, a PhD student at UCF Orlando, currently working on my dissertation

I seek your guidance in obtaining permission to include my previously published work,
[Manoj Prabakar Sargunaraj, Marcel Otto, Ladislav Vesely, Erik Fernandez, Jayanta Kapat, Valerio Viti, Swati Saxena, "Aerodynamics and Heat Transfer Investigation of Supercritical Carbon Dioxide Multi Jet Impingement Cooling for a Leading Edge at Hypersonic Speeds", AIAA SCITECH 2023 Forum, 2023,

Manoj Prabakar Sargunaraj, Marcel Otto, Ladislav Vesely, Erik Fernandez, Jayanta S. Kapat, Valerio Viti, " Use of Supercritical CO Impingement Cooling for a Hypersonic Leading Edge ", AIAA SCITECH 2022 Forum, 2022], in my dissertation. I am aware of the need to comply with copyright regulations and am willing to follow the necessary procedures.

Your assistance in this matter is crucial, and I am ready to provide any required information promptly.

Thank you for your time and support.

Sincerely,

Retention: UCF Delete after 10 Years (10 years) Expires: Mon 11/14/2033 9:15 AM

KB Katrina Buckley <KatB@aiaa.org>
To: Manoj Prabakar Sargunaraj
Cc: Kim Grant <kimg@aiaa.org>
Fri 11/17/2023 9:15 AM

Hello,
Thank you for your inquiry. Yes, you have permission to reuse all or parts of the papers in your dissertation. Please acknowledge within the main text or a footnote that relevant sections/chapters of your dissertation are reprinted with permission (e.g., "From [paper title and authors]; reprinted by permission of the American Institute of Aeronautics and Astronautics, Inc."). Note that the original source should be cited in full in the reference list.

Best,

Katrina Buckley
Managing Editor, Books

American Institute of Aeronautics and Astronautics www.aiaa.org
12700 Sunrise Valley Drive, Suite 200
Reston, VA 20191-5807
800-639-AIAA (2422)
katb@aiaa.org 703.264.7666 (direct)

REFERENCES

[1] S.D. Kasen, Thermal Management at Hypersonic Leading Edges, University of Virginia, 2013.

[2] S.D. Kasen, H.N.G. Wadley, Heat Pipe Thermal Management at Hypersonic Vehicle Leading Edges: A Low-Temperature Model Study, J Therm Sci Eng Appl. 11 (2019) 1–12. https://doi.org/10.1115/1.4042988.

[3] M. MacLean, E. Marineau, R. Parker, M. Holden, A. Dufrene, P. DesJardin, Effect of surface catalysis on measured heat transfer in expansion tunnel facility, J Spacecr Rockets. 50 (2013) 470–474. https://doi.org/10.2514/1.A32327.

[4] S. Deep, G. Jagadeesh, Gas-Surface Energy Exchange Characterization Around a Cone in the Free-Piston-Driven Shock Tunnel, J Thermophys Heat Trans. (2021) 1–16. https://doi.org/10.2514/1.t6016.

[5] J.C. Han, Fundamental gas turbine heat transfer, J Therm Sci Eng Appl. 5 (2013) 1–15. https://doi.org/10.1115/1.4023826.

[6] X.W. Zhu, J.Q. Zhao, Study on helium impingement cooling for a sharp leading edge subject to aerodynamic heating, Appl Therm Eng. 107 (2016) 253–263. https://doi.org/10.1016/j.applthermaleng.2016.06.013.

[7] P. Dechaumphai, E.A. Thornton, A.R. Wieting, Flow-thermal-structural study of aerodynamically heated leading edges, J Spacecr Rockets. 26 (1989) 201–209. https://doi.org/10.2514/3.26055.

[8] G. V. Shoev, Y.A. Bondar, G.P. Oblapenko, E. V. Kustova, Development and testing of a numerical simulation method for thermally nonequilibrium dissociating flows in ANSYS Fluent, Thermophysics and Aeromechanics. 23 (2016) 151–163. https://doi.org/10.1134/S0869864316020013.

[9] M.P. Sargunaraj, M. Otto, L. Vesely, E. Fernandez, J. Kapat, V. Viti, Use of Supercritical CO2 Impingement Cooling for a Hypersonic Leading Edge, AIAA Science and Technology Forum and Exposition, AIAA SciTech Forum 2022. (2022) 1–14. https://doi.org/10.2514/6.2022-0266.

[10] V. Viti, K. Zore, A. Jain, S. Gao, J.-S. Cagnone, J. Stokes, L. Zori, Thermal Non-equilibrium and Conjugate Heat Transfer Effects for Four Canonical Hypersonic Test Cases: Numerical Validation and Analysis, (2021) 1–21. https://doi.org/10.2514/6.2021-2506.

[11] N. Adhikari, A. Alexeenko, Development and Verification of Nonequilibrium Reacting Airflow Modeling in ANSYS Fluent, J Thermophys Heat Trans. (2021) 1–11. https://doi.org/10.2514/1.t6271.

[12] M.P. Sargunaraj, M. Otto, L. Vesely, E. Fernandez, J. Kapat, V. Viti, S. Saxena, Aerodynamics and Heat Transfer Investigation of Supercritical Carbon Dioxide Multi Jet Impingement Cooling for a Leading Edge at Hypersonic Speeds, n.d.

[13] J.D. Anderson, Hypersonic and High Temperature Gas Dynamics, (AIAA Educ, American Institute of Aeronautics and Astronautics, 2006.

[14] B. Chang, J. Huang, W.X. Yao, Thermal Protection Mechanism of a Novel Adjustable Non-Ablative Thermal Protection System for Hypersonic Vehicles, Aerospace. 10 (2023). https://doi.org/10.3390/aerospace10010001.

[15] N. He, C. Liu, Y. Pan, J. Liu, Progress of Coupled Heat Transfer Mechanisms of Regenerative Cooling System in a Scramjet, Energies (Basel). 16 (2023). https://doi.org/10.3390/en16031025.

[16] S. Luo, Z. Miao, J. Liu, J. Song, W. Xi, C. Liu, Effects of Coolants of Double Layer Transpiration Cooling System in the Leading Edge of a Hypersonic Vehicle, Front Energy Res. 9 (2021). https://doi.org/10.3389/fenrg.2021.756820.

[17] C. Yuan, J. Li, Z. Jiang, H. Yu, Experimental investigation of liquid film cooling in hypersonic flow, Physics of Fluids. 31 (2019). https://doi.org/10.1063/1.5088024.

[18] R.L. Brown, K. Das, P.G.A. Cizmas, J.D. Whitcomb, Numerical Investigation of Actively Cooled Structures in Hypersonic Flow, J Aircr. 51 (2014). https://doi.org/10.2514/1.C032394.

[19] D. Han, J.S. Kim, K.H. Kim, Conjugate thermal analysis of X-51A-like aircraft with regenerative cooling channels, Aerosp Sci Technol. 126 (2022). https://doi.org/10.1016/j.ast.2022.107614.

[20] W.H. Heiser, D.T. Pratt, Hypersonic airbreathing propulsion, American Institute of Aeronautics and Astronautics, 1994.

[21] Jr., Frederick S. Billig and Stephen E. Grenleski, COOLED LEADING EDGE, United States Patent Office. US3369782 (1968).

[22] S. V. Ekkad, P. Singh, A modern review on jet impingement heat transfer methods, J Heat Transfer. 143 (2021) 1–15. https://doi.org/10.1115/1.4049496.

[23] R. Ding, J. Wang, F. He, M. Wang, Y. Luan, G. Dong, L. Tang, Numerical investigation on a double layer combined cooling structure for aerodynamic heat control of hypersonic vehicle leading edge, Appl Therm Eng. 169 (2020) 114949. https://doi.org/10.1016/j.applthermaleng.2020.114949.

[24] S. Luo, Z. Miao, J. Liu, J. Song, W. Xi, C. Liu, Effects of Coolants of Double Layer Transpiration Cooling System in the Leading Edge of a Hypersonic Vehicle, Front Energy Res. 9 (2021). https://doi.org/10.3389/fenrg.2021.756820.

[25] A. Hadipour, M. Rajabi Zargarabadi, Heat transfer and flow characteristics of impinging jet on a concave surface at small nozzle to surface distances, Appl Therm Eng. 138 (2018) 534–541. https://doi.org/10.1016/j.applthermaleng.2018.04.086.

[26] F. Vehicles, H.J. Gladden, M.E. Melis, T.T. Mockler, M. Tong, S. Technology, Thermal/Structural Analyses of Several Hydrogen-Cooled Leading-Edge Concepts, (1990).

[27] M.E. Melis, Multiphysics Simulation of Active Hypersonic Cowl Lip Cooling, 1999.

[28] D.E. Clemons, J.M. Brupbacher, M.C. Brupbacher, W.M. Buchta, K.S. Caruso, D.E. King, D.C. Nagle, D. Zhang, Multifunctional Hypersonic Components and Structures, 2021. www.jhuapl.edu/techdigest.

[29] J.R.M.B.F.H.C. von S.D.D.M.H.O.J.H.B.E.& A.G. Torben Fiedler, Mechanical Integrity of Thermal Barrier Coatings: Coating Development and Micromechanics, 2020. http://www.springer.com/series/4629.

[30] F. Cernuschi, P. Bison, Thirty Years of Thermal Barrier Coatings (TBC), Photothermal and Thermographic Techniques: Best Practices and Lessons Learned, Journal of Thermal Spray Technology. 31 (2022) 716–744. https://doi.org/10.1007/s11666-022-01344-w.

[31] I. Barwinska, M. Kopec, D. Kukla, C. Senderowski, Z.L. Kowalewski, Thermal Barrier Coatings for High-Temperature Performance of Nickel-Based Superalloys: A Synthetic Review, Coatings. 13 (2023). https://doi.org/10.3390/coatings13040769.

[32] Y. Zhao, H. Huang, Numerical study of hypersonic surface heat flux with different air species models, Acta Astronaut. 169 (2020) 84–93. https://doi.org/10.1016/j.actaastro.2020.01.002.

[33] Q. Niu, Z. Yuan, S. Dong, H. Tan, Assessment of nonequilibrium air-chemistry models on species formation in hypersonic shock layer, Int J Heat Mass Transf. 127 (2018) 703–716. https://doi.org/10.1016/j.ijheatmasstransfer.2018.07.007.

[34] G. Shoev, G. Oblapenko, O. Kunova, M. Mekhonoshina, E. Kustova, Validation of vibration-dissociation coupling models in hypersonic non-equilibrium separated flows, Acta Astronaut. 144 (2018) 147–159. https://doi.org/10.1016/j.actaastro.2017.12.023.

[35] M.E. Holloway, R.S. Chaudhry, I.D. Boyd, Assessment of Hypersonic Double-Cone Experiments for Validation of Thermochemistry Models, J Spacecr Rockets. 59 (2021) 1–12. https://doi.org/10.2514/1.a35052.

[36] J. Hao, J. Wang, C. Lee, Numerical simulation of high-enthalpy double-cone flows, AIAA Journal. 55 (2017) 2471–2475. https://doi.org/10.2514/1.J055746.

[37] G. V. Candler, Rate Effects in Hypersonic Flows, Annu Rev Fluid Mech. 51 (2019) 379–402. https://doi.org/10.1146/annurev-fluid-010518-040258.

[38] X. Yang, G. Xiao, Y. Du, L. Liu, D. Wei, Y. Gui, Heat transfer with interface effects in high-enthalpy and high-speed flow: Modelling review and recent progress, Appl Therm Eng. 195 (2021). https://doi.org/10.1016/j.applthermaleng.2021.116721.

[39] J. YANG, M. LIU, Numerical analysis of hypersonic thermochemical non-equilibrium environment for an entry configuration in ionized flow, Chinese

Journal of Aeronautics. 32 (2019) 2641–2654. https://doi.org/10.1016/j.cja.2019.06.004.

[40] N. Adhikari, A. Dissertation, INVESTIGATION OF AEROTHERMODYNAMIC AND CHEMICAL KINETIC MODELS FOR HIGH-SPEED NONEQUILIBRIUM FLOWS, 2021.

[41] L. Gao, X.C. Zhao, B. Wang, Thermostructural responses of metallic lattice-frame sandwich structure for hypersonic leading edges, J Thermophys Heat Trans. 35 (2021) 708–714. https://doi.org/10.2514/1.T6197.

[42] L. Hongpeng, L. Weiqiang, Thermal-structural analysis of the platelet heat-pipe-cooled leading edge of hypersonic vehicle, Acta Astronaut. 127 (2016) 13–19. https://doi.org/10.1016/j.actaastro.2016.05.014.

[43] Fluent Thoery Guide, Ansys Fluent Theory Guide, ANSYS Inc., USA. 15317 (2013) 724–746. http://scholar.google.com/scholar?hl=en&btnG=Search&q=intitle:ANSYS+FLUENT+Theory+Guide#0.

[44] Ansys, ANSYS FLUENT User' s Guide, Knowledge Creation Diffusion Utilization. 15317 (2012) 724–746.

[45] S.M. Prabakar, T.M. Muruganandam, Experimental investigations of a diffuser start / unstart characteristics for two stream supersonic wind tunnel, (n.d.).

[46] S.M. Prabakar, C. Srikanth, T.M. Muruganandam, Effect of Mach Number on Shock Oscillations in Supersonic Diffusers, (2017). https://doi.org/10.1007/978-3-319-46213-4.

[47] N. Raju, M.P. Sargunaraj, B. Medhi, T.M. Muruganandam, Three dimensional schlieren using iterative phase tomography, in: AIAA Scitech 2020 Forum, 2020. https://doi.org/10.2514/6.2020-2205.

[48] N. Raju, M. Prabakar, B. Medhi, M. Osborn Oliver, T.M. Muruganandam, Tomographic schlieren system for visualisation of supersonic jet, in: 54th AIAA Aerospace Sciences Meeting, American Institute of Aeronautics and Astronautics Inc, AIAA, 2016. https://doi.org/10.2514/6.2016-1050.

[49] S. Manoj Prabakar, L.M. Panchabudhe, T.M. Muruganandam, T. Sundararajan, A study on the performance characteristics of two-stream supersonic diffusers, Aerosp Sci Technol. 95 (2019). https://doi.org/10.1016/j.ast.2019.105470.

[50] N. Raju, M.P. Sargunaraj, B. Medhi, T.M. Muruganandam, Three dimensional schlieren using iterative phase tomography, in: AIAA Scitech 2020 Forum, American Institute of Aeronautics and Astronautics Inc, AIAA, 2020. https://doi.org/10.2514/6.2020-2205.

[51] W. Zhao, X. Yang, J. Wang, Y. Zheng, Y. Zhou, Evaluation of Thermodynamic and Chemical Kinetic Models for Hypersonic and High-Temperature Flow Simulation, Applied Sciences (Switzerland). 13 (2023). https://doi.org/10.3390/app13179991.

[52] C. Park, Review of chemical-kinetic problems of future NASA missions, I: Earth entries, in: J Thermophys Heat Trans, American Institute of Aeronautics and Astronautics Inc., 1993: pp. 385–398. https://doi.org/10.2514/3.431.

[53] P.A. Gnoffo, R.N. Gupta, J.L.- Shinn, Conservation Equations and Physical Models for Hypersonic Air Flows in Thermal and Chemical Nonequilibrium, 1989.

[54] J. Hao, J. Wang, C. Lee, Numerical study of hypersonic flows over reentry configurations with different chemical nonequilibrium models, Acta Astronaut. 126 (2016) 1–10. https://doi.org/10.1016/j.actaastro.2016.04.014.

[55] H. Jiang, J. Liu, S. Luo, W. Huang, J. Wang, M. Liu, Thermochemical non-equilibrium effects on hypersonic shock wave/turbulent boundary-layer interaction, Acta Astronaut. 192 (2022) 1–14. https://doi.org/10.1016/j.actaastro.2021.12.010.

[56] A.G. Every, Z.N. Utegulov, I.A. Veres, Pulsed laser generation of ultrasound in a metal plate between the melting and ablation thresholds, in: AIP Conf Proc, American Institute of Physics Inc., 2015: pp. 1350–1359. https://doi.org/10.1063/1.4914749.

[57] G. Grimvall, M. Thiessen, A. Ferna ndez Guillermet, Thermodynamic properties of tungsten, 1987.

[58] K. Chen, R.N. Xu, P.X. Jiang, Experimental Investigation of Jet Impingement Cooling with Carbon Dioxide at Supercritical Pressures, J Heat Transfer. 140 (2018) 1–10. https://doi.org/10.1115/1.4038421.

[59] K. Chen, R.N. Xu, P.X. Jiang, Experimental study of jet impingement boiling cooling with CO2 at subcritical pressures and comparisons with at supercritical pressures, Int J Heat Mass Transf. 165 (2021) 120605. https://doi.org/10.1016/j.ijheatmasstransfer.2020.120605.

[60] K. Chen, R.N. Xu, P.X. Jiang, Numerical investigation of jet impingement cooling of a low thermal conductivity plate by supercritical pressure carbon dioxide, Int J Heat Mass Transf. 124 (2018) 1003–1010. https://doi.org/10.1016/j.ijheatmasstransfer.2018.04.003.

[61] J.A. FAY, F.R. RIDDELL, Theory of Stagnation Point Heat Transfer in Dissociated Air, Journal of the Aerospace Sciences. 25 (1958) 73–85. https://doi.org/10.2514/8.7517.

[62] L. LEES, Laminar Heat Transfer Over Blunt-Nosed Bodies at Hypersonic Flight Speeds, Journal of Jet Propulsion. 26 (1956) 259–269. https://doi.org/10.2514/8.6977.

[63] C. Dang, K. Cheng, J. Fan, Y. Wang, J. Qin, G. Liu, Performance analysis of fuel vapor turbine and closed-Brayton-cycle combined power generation system for hypersonic vehicles, Energy. 266 (2023). https://doi.org/10.1016/j.energy.2022.126426.

[64] H. Miao, Z. Wang, Y. Niu, Performance analysis of cooling system based on improved supercritical CO2 Brayton cycle for scramjet, Appl Therm Eng. 167 (2020). https://doi.org/10.1016/j.applthermaleng.2019.114774.

[65] X. Ma, P. Jiang, Y. Zhu, Performance analysis and dynamic optimization of integrated cooling and power generation system based on supercritical CO2 cycle for turbine-based combined cycle engine, Appl Therm Eng. 215 (2022). https://doi.org/10.1016/j.applthermaleng.2022.118867.

[66] K. Cheng, J. Qin, H. Sun, H. Li, S. He, S. Zhang, W. Bao, Power optimization and comparison between simple recuperated and recompressing supercritical carbon dioxide Closed-Brayton-Cycle with finite cold source on hypersonic vehicles, Energy. 181 (2019) 1189–1201. https://doi.org/10.1016/j.energy.2019.06.010.

[67] M. Marchionni, G. Bianchi, S.A. Tassou, Review of supercritical carbon dioxide (sCO2) technologies for high-grade waste heat to power conversion, SN Appl Sci. 2 (2020). https://doi.org/10.1007/s42452-020-2116-6.